ANNUAL REVIEWS

Annual Review of Earth and Planetary Sciences

Hydrotectonics of Grand Canyon Groundwater

L.J. Crossey,[1] K.E. Karlstrom,[1] B. Curry,[1] C. McGibbon,[1] C. Reed,[1] J. Wilgus,[1,2] C.J. Whyte,[3] and T. Darrah[3]

[1]Department of Earth and Planetary Sciences, University of New Mexico, Albuquerque, New Mexico, USA; email: kek1@unm.edu

[2]Current affiliation: Sandia National Laboratories, Carlsbad, New Mexico, USA

[3]School of Earth Sciences, The Ohio State University, Columbus, Ohio, USA

Annu. Rev. Earth Planet. Sci. 2024. 52:521–47

First published as a Review in Advance on February 21, 2024

The *Annual Review of Earth and Planetary Sciences* is online at earth.annualreviews.org

https://doi.org/10.1146/annurev-earth-080723-083513

Keywords

Grand Canyon, hydrogeology, stable isotopes, fault conduits, induced seismicity

Abstract

The Grand Canyon provides a deeply dissected view of the aquifers of the Colorado Plateau and its public and tribal lands. Stacked sandstone and karst aquifers are vertically connected by a network of faults and breccia pipes creating a complex groundwater network. Hydrochemical variations define structurally controlled groundwater sub-basins, each with main discharging springs. North Rim (N-Rim), South Rim (S-Rim), and far-west springs have different stable isotope fingerprints, reflecting different mean recharge elevations. Variation within each region reflects proportions of fast/slow aquifer pathways. Often considered perched, the upper Coconino (C) aquifer has a similar compositional range as the regional Redwall-Muav (R-M) karst aquifer, indicating connectivity. Natural and anthropogenic tracers show that recharge can travel 2 km vertically and tens of kilometers laterally in days to months via fracture conduits to mix with older karst baseflow. Six decades of piping N-Rim water to S-Rim Village and infiltration of effluent along the Bright Angel fault have sustained S-Rim groundwaters and likely induced S-Rim microseismicity. Sustainable groundwater management and uranium mining threats require better monitoring and application of hydrotectonic concepts.

- Hydrotectonic concepts include distinct structural sub-basins, fault fast conduits, confined aquifers, karst aquifers, upwelling geothermal fluids, and induced seismicity.

- N-Rim, S-Rim, and far-west springs have different stable isotope fingerprints reflecting different mean recharge elevations and residence times.
- The upper C and lower R-M aquifers have overlapping stable isotope fingerprints in a given region, indicating vertical connectivity between aquifers.
- S-Rim springs and groundwater wells are being sustained by ~60 years of piping of N-Rim water to S-Rim, possibly inducing seismicity.

INTRODUCTION

Long-flowpath aquifer systems provide vital water resources for continental-scale arid regions that commonly include Indigenous communities and endemic ecosystems. In such systems, tensions about use and ongoing threats to groundwater have been exacerbated by industrialization, population growth, and climate change. Examples include the Great Artesian Basin of Australia (Keppel et al. 2019, Ordens et al. 2020), the Nubian system of Northern Africa (Mohammed et al. 2022), and the greater Colorado Plateau of the western United States (Crossey et al. 2009). Early hydrologic studies often invoked regionally simple (sandbox-type) aquifers and piston flow models that smoothly connected distant recharge to interconnected springs and wells. More realistic approaches attempt to understand hydrotectonic influences on groundwater such as partitioned structural sub-basins, multi-permeability systems of fast/slow conduits, and mixtures of young recharge with old water, including small-volume but geochemically potent upwelling of geothermal fluids that impact water quality (Crossey et al. 2016). The greater Colorado Plateau region was not included in the 10-year groundwater quality US Geological Survey (USGS) study (Belitz et al. 2022) due to low population density, but it is of outsized importance for developing present and future water equity for the public and tribal lands of the 11 associated tribes surrounding Grand Canyon National Park (GCNP) and the Baaj Nwaavjo I'tah Kukveni—Ancestral Footprints of the Grand Canyon National Monument (designated in 2023). In these high-elevation arid regions, the groundwater system also supports culturally significant springs and ecosystems that host endemic species (Kreamer et al. 2015, Stevens 2023). This review deals with ways hydrotectonic concepts can provide better understanding of groundwaters of the Colorado Plateau region that, along with reallocation of Colorado River surface water, is needed to help redress equitable water use and sustainability and provide motivation for establishing a more robust monitoring baseline for sustainable and collaborative water resource management.

The 1.6-km-deep Grand Canyon (both a World Heritage and a World Geoheritage site) lays bare the aquifer stratigraphy and fault network that underlies the Colorado Plateau. Springs that emerge from both north and south sides of the canyon provide the baseflow for all the perennial side stream tributaries. These regional inputs add significantly to Colorado River volume (Miller et al. 2016, Swanson et al. 2021) (**Figure 1**) and also cause tectonic salinization of surface waters that degrade water quality (Rumsey et al. 2017). This review presents a synthesis of stable isotope data combined with other geochemical tracers to understand flowpaths and hydrologic mixing of different water sources and pathways. The scarcity of deep wells combined with multiple recharge elevations, long flowpaths, stacked aquifers, and complex mixing of water types is such that models of regional groundwater supply and quality remain underconstrained and groundwater resources for tribal communities and sensitive ecosystems hosting endemic species remain vulnerable. Questions addressed in this review, also relevant to other aquifers, include the role of faults as fast conduits, the degree of connectivity between upper and lower semiconfined aquifers, and the extent of segmentation of hydrological sub-basins.

PREVIOUS WORK AND BACKGROUND

Advances in Grand Canyon stratigraphy and geomorphology have a more than 150-year-long history (e.g., McKee 1969, Karlstrom et al. 2014) that has led to International Union of Geological Sciences Geoheritage recognition (Karlstrom & Crossey 2023). Hydrologic studies, if somewhat less extensive, also offer potential for fundamental advances. John Wesley Powell

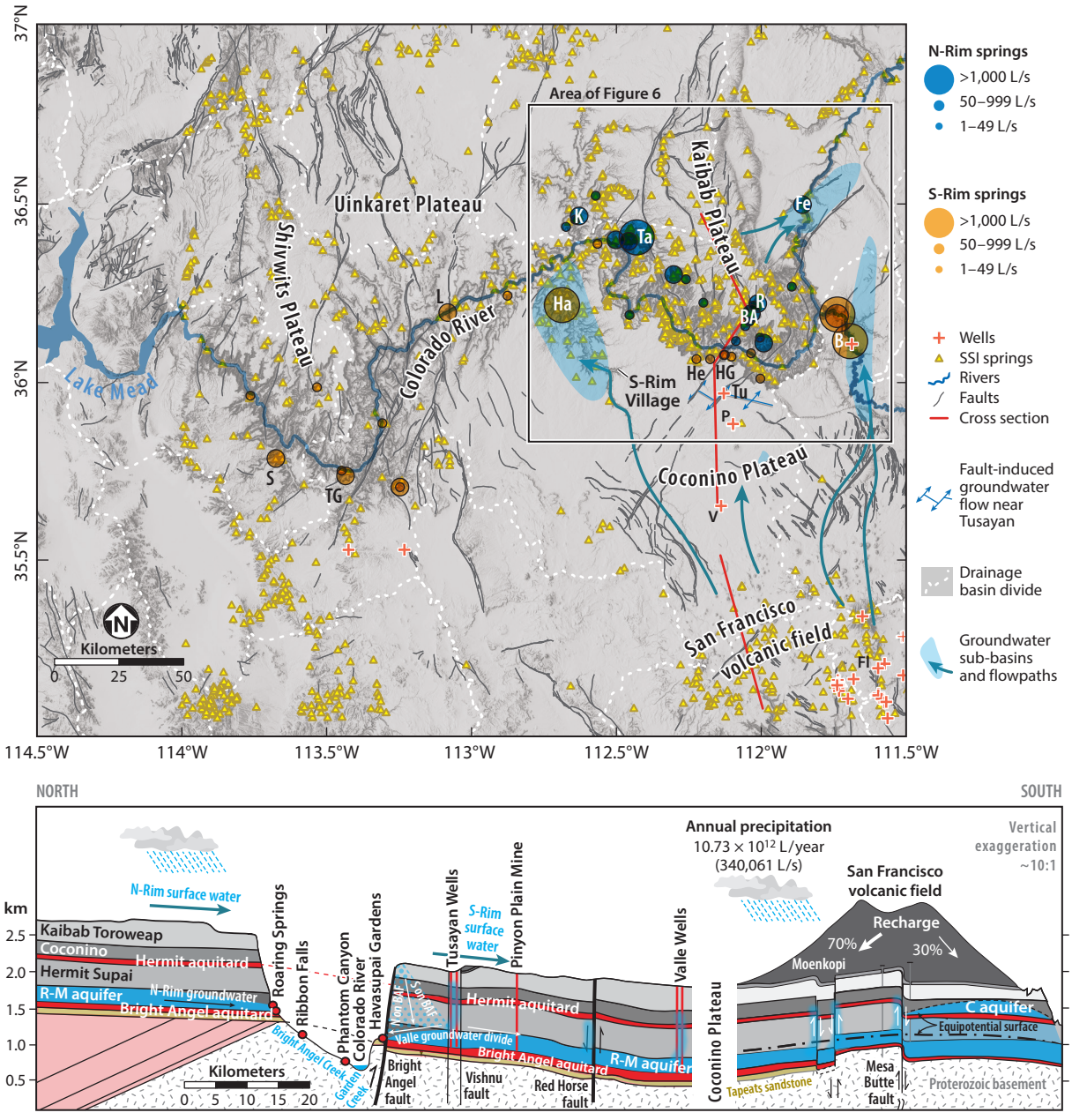

(Caption appears on following page)

Figure 1 (*Figure appears on preceding page*)

(*a*) Springs and wells of the Grand Canyon region: blue = N-Rim springs, orange = S-Rim springs, yellow triangles = minor springs from the SSI, red crosses = groundwater wells. The highest-discharge spring systems and selected locations are shown. Gray lines = faults from Billingsley and colleagues (Billingsley & Hampton 2000; Billingsley & Priest 2013; Billingsley & Workman 2000; Billingsley et al. 2003, 2006a,b, 2007, 2008, 2013). The second-order drainage divides are white dashed lines (from USGS 2018). Light blue = hypothesized fault-bounded R-M aquifer hydrologic sub-basins with high-volume springs. (*b*) N-S cross section showing C and R-M aquifers and underlying confining layers (*red*); equipotential surfaces are adapted from Errol L. Montgomery & Assoc. (1999), Crossey et al. (2009), and Curry et al. (2023). The fault-influenced groundwater divide near Tusayan is from Kessler (2002) and Crossey et al. (2009). Abbreviations: B, Blue; BA, Bright Angel; C, Coconino; Fe, Fence; Fl, Flagstaff; Ha, Havasu; He, Hermit; HG, Havasupai Gardens; K, Kanab; L, Lava; N-Rim, North Rim; P, Pinyon; R, Roaring; R-M, Redwall-Muav; S, Spencer; S-Rim, South Rim; SSI, Spring Stewardship Institute; Ta, Tapeats; TG, Travertine Grotto; Tu, Tusayan; USGS, US Geological Survey; V, Valle; WRP, Water Reclamation Plant.

famously predicted that watershed divides rather than surveyed political boundaries should be used for sustainable and equitable development of the western United States (Stegner 1992), but the opposite approach has led to political and legal wrangling over overestimated and poorly understood water resources. GCNP and surrounding communities on the Colorado Plateau rely on groundwater with increasing evidence that water supply and quality are threatened by regional development such that the well-exposed incised aquifer system in the Grand Canyon offers insights of direct applicability to uranium mining, other threats, and sustainability of springs and groundwater (Grand Canyon Trust 2023).

Early hydrologic studies centered around water supply for the growing GCNP and South Rim (S-Rim) communities. From 1901 to 1927 water was delivered by railroad (Natl. Park Serv. 1995). In 1932, a pumphouse was built to lift 6.6 L/s from Indian Gardens spring (renamed Havasupai Gardens in 2022) ∼840 m to S-Rim water storage tanks to serve S-Rim water needs. Metzger (1961) discussed S-Rim water supply as part of a then-developing transcanyon pipeline effort. Johnson & Sanderson (1968) presented some of the first hydrochemical data. From 1956 to 1966, the transcanyon pipeline was built to transfer water 20 km via gravity flow from Roaring Springs near North Rim (N-Rim) (1,585 m elevation) to Havasupai Gardens (1,150 m), where it is pumped the remaining distance to S-Rim (1,980 m). An improved 1970s pipeline moved about 17.5 L/s and, as of 1995, about 44 L/s (Natl. Park Serv. 1995). Frequent leaks and breakages along the pipeline have led to a new water supply system design that is in progress (Grand Canyon Natl. Park 2023).

Grand Canyon region hydrostratigraphy consists of an upper N aquifer in the Jurassic Navajo Sandstone and related erg deposits (Cooley et al. 1969) that exchange water with Lake Powell and supply numerous tribal communities. These and other Mesozoic rocks are being eroded back from the rims of the Grand Canyon to form the Grand Staircase (Doelling et al. 2000), leaving the 50–350-m-thick Coconino (C) aquifer consisting of the Kaibab Limestone, which forms the rim of the Grand Canyon, underlain by Toroweap Formation, Coconino Sandstone, and upper Supai Group sandstones, with aquitards in the Hermit Formation and lower Supai Group (Bills et al. 2007, Tobin et al. 2018) (**Figure 1*b***). A deeper regional karst aquifer is the Redwall-Muav (R-M) aquifer that consists of Redwall Limestone, Temple Butte Formation, and Muav Limestone that thicken from about 300 m in the east to 600 m in the west, underlain by the relatively impermeable Cambrian Bright Angel Shale (Metzger 1961; Huntoon 1968, 1970, 1974, 1982) (**Figure 1*b***).

Huntoon (1981, 2000) emphasized multi-permeability pathways within the aquifers and presented a hydrotectonic framework that we support and expand upon here. This consists of a 3D fault conduit system presently undergoing tectonic extension that allows partial connectivity of the different aquifers. A water chemistry synthesis of S-Rim Grand Canyon springs and wells was done by Monroe et al. (2005) and Bills et al. (2000, 2007). Crossey et al. (2006, 2009)

reinvigorated thinking about fault pathways and used gas chemistry data, including $^{3}He/^{4}He$, to argue that carbonic springs of the Grand Canyon contain mantle-derived fluids and significant endogenic CO_2 from magmatic sources (Crossey et al. 2006, 2016). This led to the distinction between epigenic (upper world) springs that are cold (13–17°C), have low total dissolved solids (TDS) (<350 mg/L), and provide the best drinking water. In contrast, endogenic (lower world) springs are warm (22–31°C), have higher TDS (≫350 mg/L), and are highly carbonic (CO_2 rich; alkalinities over 2,000 mg/L as HCO_3), resulting in hypogene cave dissolution (Polyak et al. 2017) and extensive travertine deposition at the surface (Crossey & Karlstrom 2012). Variable mixing of these different water sources influences the observed water chemistry variations between springs.

Stable isotope data provide a tool for evaluating mixing and further characterizing spring variability, water sources, and pathways. Zukosky (1995) presented stable isotope data on many S-Rim springs, and Ingraham et al. (2001) first suggested anthropogenic effects of pipeline water on Havasupai Springs. Springer et al. (2017) used stable isotope data across western North America to conclude that groundwater is dominated by high-elevation (winter) recharge and that variability results from the mixing of local and regional recharge. USGS hydrochemical data were synthesized for both N-Rim (Beisner et al. 2017) and S-Rim springs (Beisner et al. 2020, Solder & Beisner 2020); they concluded that observed S-Rim groundwater stable isotope variability reflects mixing of different proportions of summer and winter recharge that reaches individual springs (recharge mixing), although the study-proposed end members do not encompass the observed stable isotope variability. Nevertheless, their paper made the significant contribution of proposing a higher percentage of summer recharge than previously envisioned (cf. Bills et al. 2007). In an alternative mixing model, Curry et al. (2023) suggested that mixing within and between the aquifers homogenizes recharge variability and that groundwater mixing models better encompass the data and explain isotopic variations within and between nearby springs. Curry and others (2023) also proposed that N-Rim (pipeline) water reclaimed at the S-Rim Water Reclamation Plant infiltrates down the Bright Angel and other faults and mixes with S-Rim groundwater.

Solder et al. (2020) presented groundwater age models based on ^{14}C, tritium, and noble gas data that demonstrate chemical mixing between older regional groundwaters and a younger component, but their modeled quantification of mean age relies on assumptions of piston flow pathways that do not adequately account for mixing of CO_2-rich waters containing dead endogenic carbon. Knight & Huntoon (2022) examined both N-Rim and S-Rim springs and hypothesized five separate groundwater flow subregions that drain into the Grand Canyon, although the proposed groundwater divides remain poorly constrained. Curry et al. (2023) and Beisner et al. (2023b) tested potential hydrochemical connections between the S-Rim Water Reclamation Plant and selected springs below the S-Rim and found pharmaceutical tracers. Beisner et al. (2023a) found uranium in Horn Springs below the now-inactive Orphan Uranium Mine. Overall, the combined tracer data demonstrate a young (post-early 1950s and ongoing) anthropogenically influenced groundwater component that mixes with older baseflow.

N-Rim studies included stable isotope data and time series monitoring for Roaring Springs and other springs sourced from the Kaibab uplift. Ross (2005) modeled flow through the C and R-M karst systems to take about 1 month for some recharge events. Schindel (2015) monitored Roaring Springs, the primary source for transcanyon pipeline water, and documented some <2-day event response times. Jones et al. (2018) summarized an N-Rim dye tracer study that documented far-traveled (tens of kilometer-scale), fast (weeks to months) fluid transport from sinkholes to springs. Jones et al. (2019) summarized sinkhole distribution on the Kaibab Plateau and discussed interactions of the shallow and deep karst systems. Wood et al. (2020) focused on N-Rim recharge and infiltration processes between the upper C aquifer and the R-M aquifer. McGibbon et al. (2022)

linked the Fence Springs system of Marble Canyon to Kaibab uplift recharge. Chambless et al. (2023) provided rating curves for using stream stage data to develop better discharge estimates.

These studies have led to the present understanding of Grand Canyon hydrology, which involves a resurgence in application of hydrochemical tracers and better appreciation of the complexity of multi-permeability fluid pathways and groundwater mixing. Quantifying discharge variability and contaminant transport remain major challenges for developing a robust baseline for water supply and quality.

METHODS: MULTIPLE TRACERS

Hydrochemical data were compiled from numerous sources over several decades with broad agreement across labs and years (**Supplemental Table 1**). Data used in this review are from Bills et al. (2007), Crossey et al. (2009), Curry et al. 2023, and USGS (2020). Significant uncertainty remains in discharge measurements that reflects different types of estimates, from visual to monitored, as well as significant flow variations across multiple timescales. As examples, discharge estimates for the relatively well-studied Roaring Springs tabulated by Schindel (2015) vary from 91 to 1,560 L/s with a median of ∼160–170 L/s, compared to baseflow of 510–700 L/s based on monitoring of Bright Angel Creek, the receiving stream (USGS 2020, Swanson et al. 2021, Chambless et al. 2023). Blue Spring and other springs that provide the groundwater baseflow of the Little Colorado River provide 4,848 L/s (Bills et al. 2007) to 7,236 L/s (Swanson et al. 2021). Estimates of discharge at Havasu Springs are 1,700–1,800 L/s (Bills et al. 2007). **Figure 1** plots the high-discharge springs (>1 L/s). Notably, about 90% of S-Rim discharge into the Grand Canyon is from two spring systems, Blue and Havasu springs; ∼80% of N-Rim discharge is also from two spring/creek systems, Tapeats/Thunder/Deer and Angel/Roaring/Bright Angel. Our estimate of combined spring flow gives more than 13,500 L/s (>475 cfs) groundwater discharge into the Grand Canyon, more than 8,600 L/s from the south and more than 4,900 L/s from the north, much of it from tribal lands. For hydrochemical studies, springs and/or spring-fed side streams were sampled at a variety of flow conditions. Field temperature, pH, and conductivity were recorded. Waters were investigated using different tracers: major and trace elements, stable isotopes, and $^{87}Sr/^{86}Sr$. Tritium and ^{14}C were analyzed using standard methods, referenced in each source study. New noble gas data for 10 springs are presented along with a synthesis of prior analyses in **Supplemental Table 2**.

MAJOR SPRINGS SYSTEMS AND GROUNDWATER WELLS

Important N-Rim spring groups and their discharge and percentage of N-Rim discharge include Fence (502 L/s; 10%), Roaring/Angel/Bright Angel Creek (∼600 L/s; 12%), Shinumo (190 L/s; 4%), Tapeats/Thunder River/Deer Creek (3,046 L/s; 62%), and Kanab Canyon (4 L/s; 2%). These springs are sourced from meteoric recharge from the Kaibab Plateau, and they constitute the present and future best low TDS water supply for GCNP. Because the strata dip south on the N-Rim's Kaibab uplift, both surface water and groundwater flow south toward the canyon (**Figure 1*b***). Interconnected fault and karst networks feed springs that emerge in tributary canyons well away from the river to form perennial streams (**Figure 1**). Most N-Rim springs discharge from the Muav Formation near the lower confining layers of the (mostly drained) ∼400-m-thick R-M aquifer where it rests on the Bright Angel Shale. In contrast, the Fence Springs system, east of the Kaibab uplift, discharges from the Redwall Limestone directly into and on both sides of the Colorado River from a confined karst-fault conduit beneath the river (Huntoon 1981), with water mainly sourced from the N-Rim (McGibbon et al. 2022). Springs of the Kanab area of N-Rim (Beisner et al. 2017) (**Figure 1**) have relatively low discharge considering their large

drainage basin area because most western Kaibab uplift groundwater is routed down the West Kaibab fault/monocline system to discharge in the Tapeats/Thunder/Deer Creek system (Knight & Huntoon 2022). Springs that discharge farther west from the Uinkaret and Shivwitts plateaus are low discharge (Wilson 2000, Wilson et al. 2022).

Approximate discharge and percentage of S-Rim spring discharge into the Grand Canyon are Blue Spring/Little Colorado River system (6,230 L/s; 72%), Havasu Springs (1,838 L/s; 21%), springs of the Hualapai Plateau of the far-western Grand Canyon (253 L/s; 3%), Lava (189 L/s; 2%), and springs below S-Rim Village (86 L/s; 1%). Blue and Havasu springs emerge from the Redwall Limestone in structural depressions on either side of the southern continuation of the Kaibab uplift in sub-basins where the R-M aquifer is fully saturated. The Blue Spring/Little Colorado River system consists of about 56 springs that emerge from the Redwall in the south (∼5,000 L/s, including 2,750 at Blue Spring) and the Muav Formation farther north [∼1,000 L/s (Loughlin & Huntoon 1983)]. These springs are in the Blue Spring graben with water sourced mainly from the eastern part of the San Francisco volcanic field and routed along the Mesa Butte fault system, and around the Gray Mountain monocline system (**Figure 1**), with some contribution from the Little Colorado River infiltration and Black Mesa groundwater basin to the east (Loughlin & Huntoon 1983). Similarly, Havasu Springs are in a syncline that collects both surface water and groundwater from the large Cataract Creek drainage basin sourced mainly from the northwestern San Francisco volcanic field. Near S-Rim Village, strata dip south, carrying surface drainage away from the canyon, but groundwater flows north to feed a necklace of springs that we refer to as S-Rim GCNP springs that emerge mainly from the Muav Formation (**Figure 1*b***) in GCNP. A groundwater divide of the R-M equipotential surface near the town of Tusayan (**Figure 1**) was depicted by Errol L. Montgomery & Assoc. (1999) and modeled by Kessler (2002) and Crossey et al. (2009) to be fault influenced. The geometry of this groundwater divide remains poorly constrained because deep groundwater wells on the Coconino Plateau south of the Grand Canyon are sparse and not well monitored in terms of available records of discharge, water levels, or hydrochemistry. Groundwater wells discussed here are shown in **Figure 1*a*** and include Valle, Tusayan, Pinyon Plain Mine, Flagstaff-area wells (Bills et al. 2000), and Hualapai Plateau wells.

STABLE ISOTOPE DATA

Stable isotope analyses (**Figure 2**) measure the $\delta^{18}O$ and $\delta^{2}H$ of the H_2O molecules to help identify different fingerprints for springs and groundwater sources, and to detect flowpath processes of evaporation, water-rock interaction, and mixing. N-Rim springs from both the C aquifer (A.W. Wood, unpublished thesis; Wood et al. 2020) and the R-M aquifer (e.g., Roaring, Tapeats) have an overlapping range of $\delta^{18}O$ values from −15 to −13 (**Figure 2*b***). The mean of the Tapeats plus Roaring systems, constituting ∼90% of N-Rim spring discharge (**Figure 2*a***), is useful as the fingerprint of N-Rim springs (−13.8, −96.3). The Fence Springs system has the most negative isotopic values and is interpreted to be derived from the highest-elevation portions of the Kaibab uplift with variation that is interpreted to reflect mixing of karst baseflow with faster-traveled meteoric recharge (McGibbon et al. 2022). Vasey's Spring system is offset from Fence about 5‰ in δD; has more variation in temperature, discharge, and composition; and is interpreted to have a higher percentage of fast-traveled recharge (McGibbon et al. 2022) similar to the explanation for Roaring Springs variability (Brown 2011).

S-Rim springs and wells also have overlapping compositions in both C and R-M aquifers with $\delta^{18}O$ values of −13 to −11, but S-Rim and N-Rim springs have distinctly different stable isotope fingerprints. The mean of the Blue/Havasu springs systems, ∼80% of S-Rim spring discharge

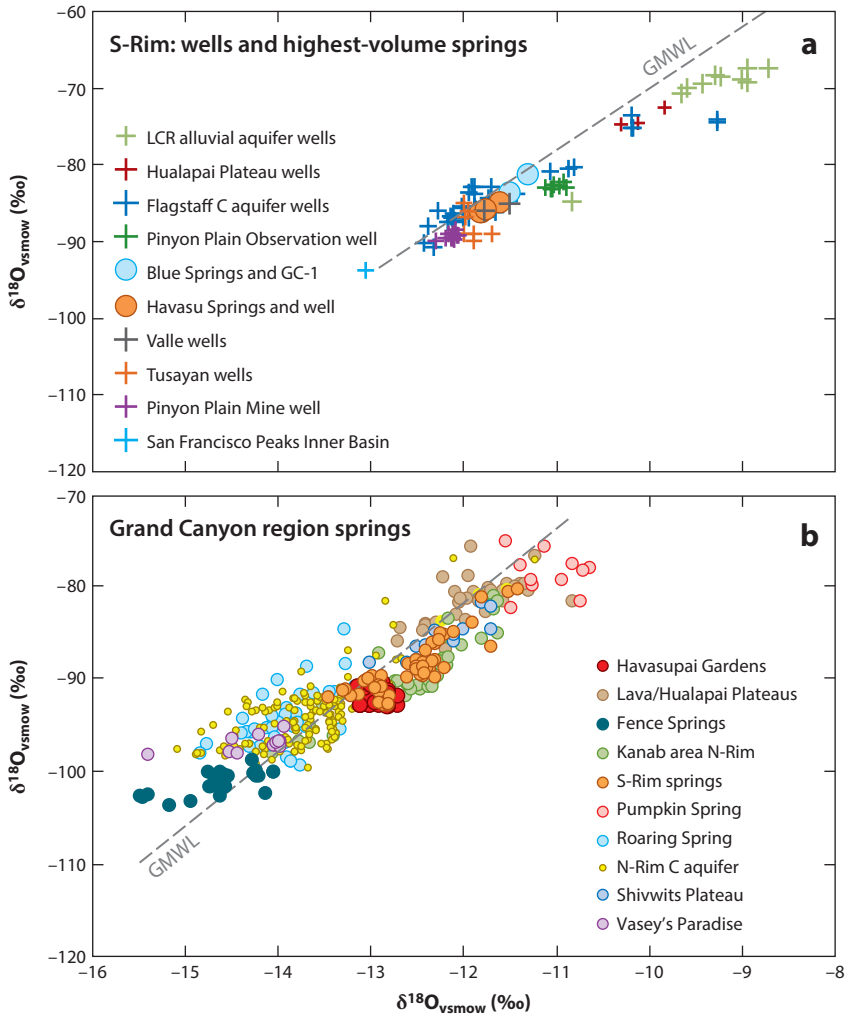

Figure 2

Stable isotopes of waters from the Grand Canyon region. (*a*) S-Rim wells showing highly variable C aquifer waters that overlap with R-M aquifer waters of the Coconino Plateau wells and with the highest-discharge springs of the Blue and Havasu springs systems. (*b*) Grand Canyon region springs showing varying fingerprints by region. Havasupai Gardens has intermediate composition between N-Rim and S-Rim springs, suggesting pipeline mixing. Springs show a west-to-east ~4‰ depletion in $\delta^{18}O$, reflecting increasing recharge elevations from the Hualapai to Coconino/Shivwitts to Kaibab/San Francisco Peaks plateaus. (*c*) Regression lines from creeks intersecting the GMWL (Craig 1961) near the likely spring-source recharge composition. (*d*) Alternative mixing models to explain groundwater variation are groundwater mixing (this review) or recharge mixing (Solder & Beisner 2020); faded small points representing winter (*blue*) and summer (*orange*) recharge. Data are in **Supplemental Table 1**. Abbreviations: B, Blue; C, Coconino; C-aqN, C aquifer from N-Rim; C-aqS, C aquifer from Coconino Plateau and Flagstaff; F, Fence, GMWL, Global Meteoric Water Line; H, Havasu; HG, Havasupai Gardens; HP, Hualapai Plateau; L, Lava; LCR, Little Colorado River; N-Rim, North Rim; PP, Pinyon Plain; R, Roaring; R-M, Redwall-Muav; S-Rim, South Rim; T, Tusayan; V, Valle; WRP, Water Reclamation Plant.

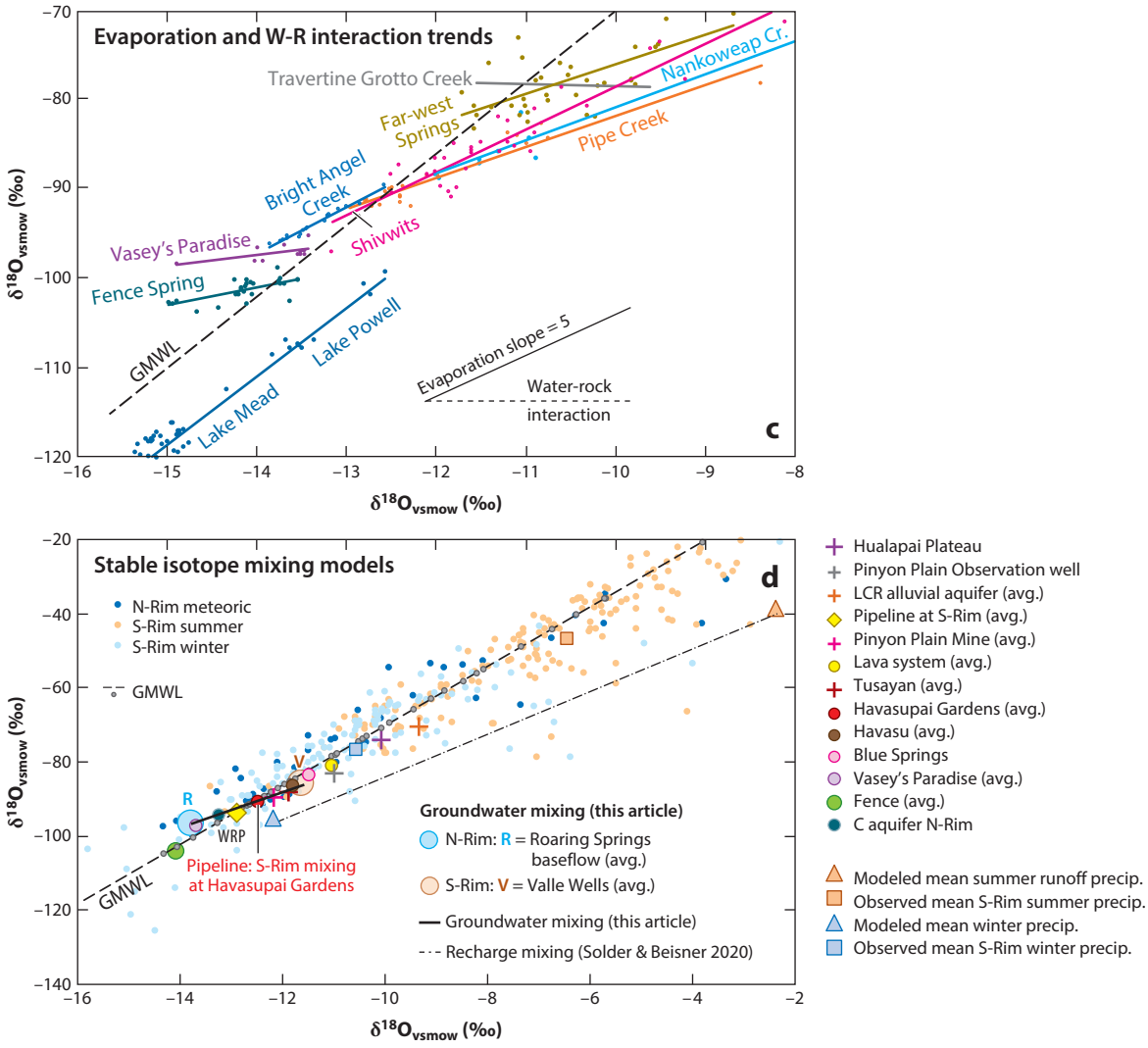

Figure 2

(*Continued*)

into the Grand Canyon, provides an S-Rim groundwater fingerprint (−11.6, −85.5). Havasupai Gardens (previously Indian Gardens), directly below S-Rim Village and along the Bright Angel fault, was reported by Lattimore et al. (1987) to have been an unreliable spring in the 1930s with a discharge of 18 L/s, but it is now one of the higher-discharge S-Rim GCNP spring systems (27.9 L/s). Havasupai Gardens waters range in $\delta^{18}O$ from about −13.6 to −12.6‰ and are the most negative among S-Rim springs and wells with the mean of Havasupai Gardens (−12.5, −92.8‰) plotting between the means of N-Rim and S-Rim waters. This suggests the possibility of mixing of N-Rim end members via anthropogenic influence of pipeline leakage and infiltration from the Water Reclamation Plant on S-Rim (Ingraham et al. 2001, Curry et al. 2023).

An alternative interpretation is that Havasupai Gardens springs is a natural end member for S-Rim groundwater mixing. But the groundwater wells on the S-Rim Coconino Plateau and the

high-volume Havasu Springs that best characterize up-gradient S-Rim water are about 1‰ less negative in $\delta^{18}O$ than Havasupai Gardens such that this interpretation would require a different source and pathway for Havasupai Gardens than for other S-Rim groundwaters, which seems unlikely. A high-elevation municipal well (IB-9) from the Inner Basin of the San Francisco Peaks has $\delta^{18}O$ of approximately −13‰ that homogenizes even more negative high-elevation snowmelt recharge from the San Francisco Peaks [$\delta^{18}O$ of approximately −16‰ (Bills et al. 2000)]. But Wupatki National Monument wells, about 30 km downslope to the northeast of the San Francisco Peaks, have $\delta^{18}O$ of −10‰ because of mixing of mountain recharge with highly ^{18}O-depleted summer runoff stored in Little Colorado alluvial aquifer wells (Mason et al. 2023) (**Figure 2*a***). Nearby Sunset Crater and Walnut Canyon National Monument wells and Flagstaff city water (Bills et al. 2000) form a group of Coconino Plateau C aquifer wells with a composition similar to Blue Spring, Valle, Tusayan, and Pinyon Plain Mine wells. Pinyon Plain Mine Observation Well in the C aquifer is less negative ($\delta^{18}O$ of about −11‰) than the deeper R-M aquifer well ($\delta^{18}O$ of about −12.2‰) at this site. However, the overall similarity in the range of stable isotopic values between the C and R-M aquifers in a given region on both the S-Rim (**Figure 2*a***) and N-Rim (**Figure 2*b***) suggests the C aquifer is connected to the R-M aquifer by vertical fault pathways.

Repeat sampling indicates that most springs have significant compositional variation along regression line segments that have lower slopes than the Global Meteoric Water Line (GMWL) (**Figure 2*b***). For the Roaring and Fence springs systems, internal variation of about 1.5‰ in $\delta^{18}O$ is interpreted to be due to mixing of R-M karst baseflow with less negative recharge water from faster-traveled pathways that has experienced some evaporation (Brown 2011, McGibbon et al. 2022). Variation along regression lines with slopes of ∼5, a slope suggesting evaporation (Sharp 2017) (**Figure 2*c***), occurs in creeks on both N-Rim (Bright Angel Creek, Nankoweap, Shivwitts) and S-Rim (Pipe, far-western springs). An additional factor is mixing with geothermal waters where water-rock interaction causes lower slopes (shift to more ^{18}O enriched at near-constant δD) (Sharp 2017). This process may also have influenced Fence, Vasey's, and Travertine Grotto where geothermal inputs are also indicated by other tracers: helium isotopes and external CO_2 (Crossey et al. 2006).

Our interpretation of the more than 2‰ difference in $\delta^{18}O$ between the stable isotope signatures of N-Rim, S-Rim, and far-western groundwater (**Figure 2*b***) is that they reflect the different average elevations of the recharge areas, 2.5 km for N-Rim Kaibab uplift, 1.9 for N-Rim Shivwits Plateau, 1.8 km for S-Rim Coconino Plateau, and 1.5 km for the far-western S-Rim Hualapai Plateau. Increasing elevation related to the Kaibab uplift explains the west-to-east progressive change to more negative stable isotope signatures on both rims. This interpretation has similarities to Springer et al. (2017), who suggested a mix of local and regional sources, and also to Solder & Beisner (2020), who emphasized seasonal variation of recharge with an important role for summer monsoonal runoff. But our emphasis is different in that we propose that aquifers homogenize precipitation within subregional-scale source plateaus. This is based on the observation that C and R-M aquifer waters (in springs and wells) have similar composition within each rim area, suggesting that recharge is homogenized in the highly fractured and only locally perched C aquifer, and there is vertical connectivity between C and R-M aquifers over time in each subregion.

Stable isotope values of precipitation on both rims are much more varied than groundwater values (**Figure 2*d***). Both rim areas are recharged by a dominance of winter recharge but with a strong influence of summer monsoons especially on S-Rim and far-western groundwater. With evaporation and geothermal mixing effects removed, means of S-Rim springs and wells fall just below the GMWL in a near-continuum of $\delta^{18}O$ values from −12 to −9‰ with pipeline-influenced S-Rim waters extending to $\delta^{18}O = -13$‰. Havasupai Gardens plots midway between N-Rim and S-Rim groundwater end members, suggesting subequal mixing between N-Rim pipeline water

(Roaring Springs baseflow end member of **Figure 2*d***) and S-Rim groundwater (Valle wells as a possible end member), and this also can explain variation of many of the S-Rim GCNP springs as proposed by Curry et al. (2023). But other waters in the continuum of values could also be considered as mixing end members with different implications for the geographic scale of mixing. Pinyon Plain Observation Well in the C aquifer is similar to some Flagstaff C aquifer values and could mix with Pinyon Plain Mine–type R-M waters such that C to R-M mixing could explain much of the S-Rim variation (except the more negative Havasupai Gardens values). Our preferred groundwater mixing model extends beyond these end members and involves groundwater mixing of fast- and slower-traveled waters on the S-Rim (**Figure 2*b***) with pipeline mixing affecting Havasupai Gardens (**Figure 2*a*,*b***) and other springs below S-Rim Village.

The alternate recharge mixing interpretation of the same stable isotope variation provided by Solder & Beisner (2020) uses proposed end members of modeled summer runoff recharge versus modeled winter recharge. In this mixing model, spring-to-spring variation is explained in terms of varying recharge proportions (expressed as F_{win}) that reach individual springs. However, their proposed recharge end members do not encompass the observed groundwater data (**Figure 2*d***). For example, Havasupai Gardens is reported to consist of 103% winter recharge, and there is no explanation for why Havasupai Gardens should have the most negative water isotopic values on the S-Rim; why it is more negative than the up-gradient Tusayan, Pinyon Plain Mine, and Valle wells; why it differs from 90% of S-Rim groundwater as reflected in Blue and Havasu springs; or why S-Rim GCNP springs that are nearby to each would gather such different recharge proportions. However, recharge variation likely does explain hydrologic sub-basin stable isotope variation with different proportions and values of summer and winter meteoric precipitation at the different mean elevations of the different plateau recharge areas.

SOLUTES AND WATER FLOWPATHS

Analysis of solutes helps decipher water-rock interactions, residence times, and groundwater mixing. Major element chemistry of springs is shown graphically in **Figure 3*a*** in the form of a Piper diagram (Piper 1944). This displays the normalized proportions of cations and anions expressed in millequivalents, a unit that accounts for both molar concentration and charge of ions. This diagram plots cations and anions as two separate triangles and also shows the ionic composition holistically in the projected parallelogram. Points are scaled for TDS, which adds to the utility of the diagram.

Large-volume springs on the N-Rim and most of the C aquifer wells near Flagstaff are upper world waters with TDS less than 350 mg/L, cool temperatures of 13–17°C, near-neutral pH values of 7–8, and a narrow solute compositional range (Bills et al. 2000, Crossey et al. 2009). They are also the lowest TDS waters in the region. This suite of waters is Ca-Mg-HCO_3-dominated freshwater that plots at the left vertex of the Piper parallelogram and is typical of snowmelt passed through limestone aquifers. In contrast, travertine-depositing lower world springs reflect a component of the water originated from deep sources, below the aquifers. These are 22–31°C, have neutral to slightly acidic pH of 6–7.5, have much higher TDS of $\gg$350 mg/L, and have exceptionally high alkalinity (up to 2,276 mg/L as HCO_3). P_{CO_2} values are more than two orders of magnitude above atmospheric or soil gas values (Crossey et al. 2006, 2016) and are interpreted to reflect magmatic CO_2 contributions carried in geothermal fluids from nearby young volcanic fields based on associated noble gas tracers and stable isotope composition.

Figure 3*a* shows several regional trends in which different high TDS lower world waters mix with the dominantly meteoric upper world end member. The Blue Spring system shows mixing of a NaCl-rich lower world end member that Loughlin & Huntoon (1983) suggested came from

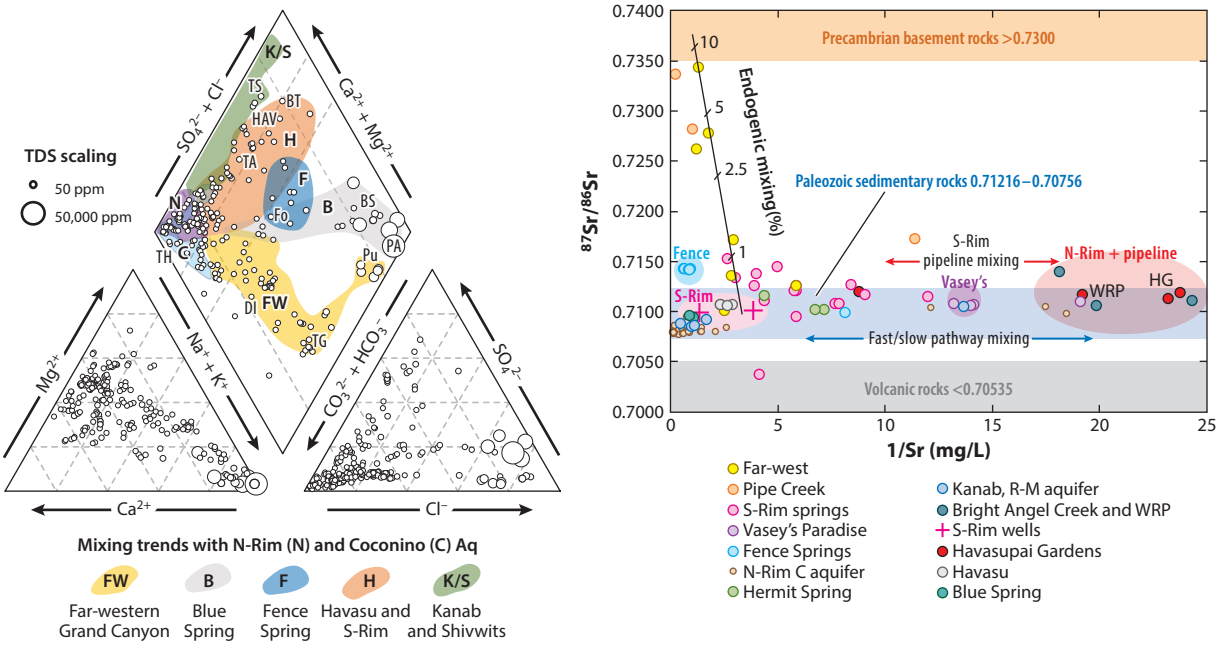

Figure 3

(*a*) Piper diagram showing solute compositions of different mixing trends. Points are from Crossey et al. (2009) with additional fields added from the literature. A near-meteoric end member is defined by N-Rim Kaibab uplift springs (Wood et al. 2020) and C aquifer wells near Flagstaff (Bills et al. 2000) at the left apex of the parallelogram. A Cl-rich mixing trend is shown with Blue Spring (gray; Loughlin & Huntoon 1983, McGibbon et al. 2022, Mason et al. 2023). A sulfate-rich mixing trend is seen throughout much of the Grand Canyon (orange and green; Beisner et al. 2017, 2020; Wilson et al. 2022). A high-sodium/high-HCO_3 mixing trend is present in the F-W Grand Canyon (yellow; Hualapai Plateau). (*b*) $^{87}Sr/^{86}Sr$ versus 1/Sr for Grand Canyon springs and wells showing several mixing trends. Abbreviations: B, Blue; BT, Blacktail; C, Coconino; Di, Diamond; F, Fence; FW, far-west; H, Havasu; K, Kanab; N-Rim, North Rim; PA, Palisades; Pu, Pumpkin; S, Shivwits; S-Rim, South Rim; TA, Tapeats; TG, Travertine Grotto; TH, Thunder River; TS, Travertine Slot.

the Black Mesa groundwater basin to the east but that also could reflect up-gradient waters of the Little Colorado River alluvial aquifer (Mason et al. 2023) and endogenic fluids of the San Francisco volcanic field. Fence Springs are similar to Blue Spring and have higher TDS than Vasey's Spring, possibly including solute inputs from the east (Huntoon 1981) and/or geothermal inputs (McGibbon et al. 2022). Havasu, other S-Rim GCNP springs, Kanab, and Shivwitts plateau springs on the N-Rim show mixing of the meteoric upper world end member with an SO_4-rich end member that most likely reflects sulfate acquired from gypsum-bearing units in the C aquifer, especially the Toroweap Formation (Beisner et al. 2017, Wilson et al. 2022) and/or a component from oxidation of magmatic sulfur (Crossey et al. 2006). A third mixing trend is shown in Lava Spring, Travertine Grotto Springs, and other far-west Hualapai Plateau springs where high-Na waters also contain high bicarbonate, perhaps related to CO_2 input along the Hurricane, Toroweap, and Lava faults. Overall, these solute data complement the stable isotope data by showing regionally distinct groundwater sub-basins, with solute variation within each sub-basin attributed to variable water-rock interaction with higher TDS acquired along the slower water pathways and with different lower world end members reflecting differing geothermal end members.

The solute Sr and its $^{87}Sr/^{86}Sr$ ratio provide a sensitive tracer of water-rock interactions and mixing (**Figure 3*b***). Sr concentration [Sr] reflects both dissolution and precipitation process along a flowpath, whereas the radiogenic composition ($^{87}Sr/^{86}Sr$) reflects the Sr source. N-Rim waters

have a wide range of [Sr] at low $^{87}Sr/^{86}Sr$ characteristic of derivation from marine limestone and reflecting variable percentages of fast (low [Sr]) and slow (high [Sr]) transit time to pick up solutes. N-Rim Kaibab uplift water (pipeline water that supplies S-Rim drinking water and the Water Reclamation Plant) has the lowest [Sr] (highest 1/[Sr]). High $^{87}Sr/^{86}Sr$ and high [Sr] at Fence suggest endogenic inputs. The Kanab area of the N-Rim has a range of [Sr] at low $^{87}Sr/^{86}Sr$ reflecting pathways in the sedimentary aquifers and shows that C and R-M aquifer waters are very similar. The high-volume Blue and Havasu springs, and the Valle and Pinyon Plain Mine wells, hence >80% of S-Rim groundwater (**Figure 3*b***), have high [Sr] and low $^{87}Sr/^{86}Sr$ suggesting long flowpaths in the sedimentary aquifers. Havasupai Gardens and Garden Creek (**Figure 2*b***) have lower [Sr] than any S-Rim water, reinforcing the interpretation that they are a mix of S-Rim groundwater with N-Rim water. Travertine Grotto and Pipe Creek waters range in composition from typical S-Rim meteoric waters to very high $^{87}Sr/^{86}Sr$ waters with high [Sr] that record mixing of 1–10% of geochemically potent geothermal waters with radiogenic Sr derived from Precambrian granites (Crossey et al. 2006, Curry et al. 2023).

NOBLE GASES AND RADIOGENIC AND COSMOGENIC ISOTOPE TRACERS

Helium isotopes and trace gas analyses have been applied to test whether waters are in equilibrium with air and the nature of any nonair-like fluid component sourced from below the aquifer system (Crossey et al. 2006, 2009; Solder et al. 2020). Grand Canyon springs fall into the same two main noble gas groupings shown by the solute data. Upper world (meteoric) waters have dissolved gases similar to air-saturated water (ASW) (low He/Ar, high N_2/Ar, and N_2/He) and are found in N-Rim springs such as Tapeats, Vasey's, and Crystal (Crossey et al. 2006) as well as the S-Rim springs potentially influenced by pipeline water including Havasupai Gardens, Horn Spring, Pipe Spring, 140-Mile, National, and Grapevine (Solder et al. 2020) (**Figure 4**). Lower world (geothermal) waters are nonair-like (elevated He/Ar and N_2/Ar, and He/Ne > 2.5) and are found in Fence, Blue, and Havasu springs, in fluids along the Palisades fault, in many carbonic travertine-depositing S-Rim springs, and in hot springs beneath and downstream of Lake Mead (Crossey et al. 2006, 2009) (**Figure 4**).

Helium isotope analyses measure R, the ratio of ^{3}He (dominantly primordial) to the much more prevalent ^{4}He isotope that is produced by radioactive decay of U and Th (an alpha particle). The *y* axis of **Figure 4** plots R/R_A, the measured $^3He/^4He$ ratio (R) divided by the $^3He/^4He$ ratio in air ($R_A \sim 1.384 \times 10^{-6}$). The *x* axis plots measured $^4He/^{20}Ne$ divided by the $^4He/^{20}Ne$ value of ASW $(^4He/^{20}Ne)_{ASW}$ that was calculated for each sample individually based on water temperature, elevation, and salinity (conductance) (Weiss 1971, Klemperer et al. 2022). Ternary mixing lines are calculated between end members of ASW (0.985, 1.0); mid-ocean ridge basalt (MORB) gas (270,000, 8.0), and crustal fluids (270,000, 0.02), quantifying mixing of air-like meteoric fluids with nonair-like fluids. The initial $(^4He/^{20}Ne)_{ASW}$ value used for the ternary mixing lines is the mean of the ASW values calculated for this data set $(^4He/^{20}Ne)_{ASW} = 0.27$. Thus, air-like fluids plot toward the left near 1 on the *x* axis, whereas nonair-like fluids plot as $\gg$1. Nonair-like fluids from the crust (**Figure 4**) record ^{4}He buildups as a consequence of radioactive decay; nonair-like mantle fluids can be from asthenospheric mantle (MORB $\sim 8\ R_A$) or subcontinental lithospheric mantle (SCLM) ($\sim 6\ R_A$). Quaternary basalts in the region are derived from a mix of asthenospheric (Crow et al. 2014) and lithospheric (Porter & Reid 2021) sources such that associated magmatic volatiles likely also have mixed mantle sources.

N-Rim epigenic springs have not been measured for helium isotopes but likely have $^3He/^4He$ near ASW ($0.985\ R_A$) with little ^{4}He addition from the crust or mantle. Numerous

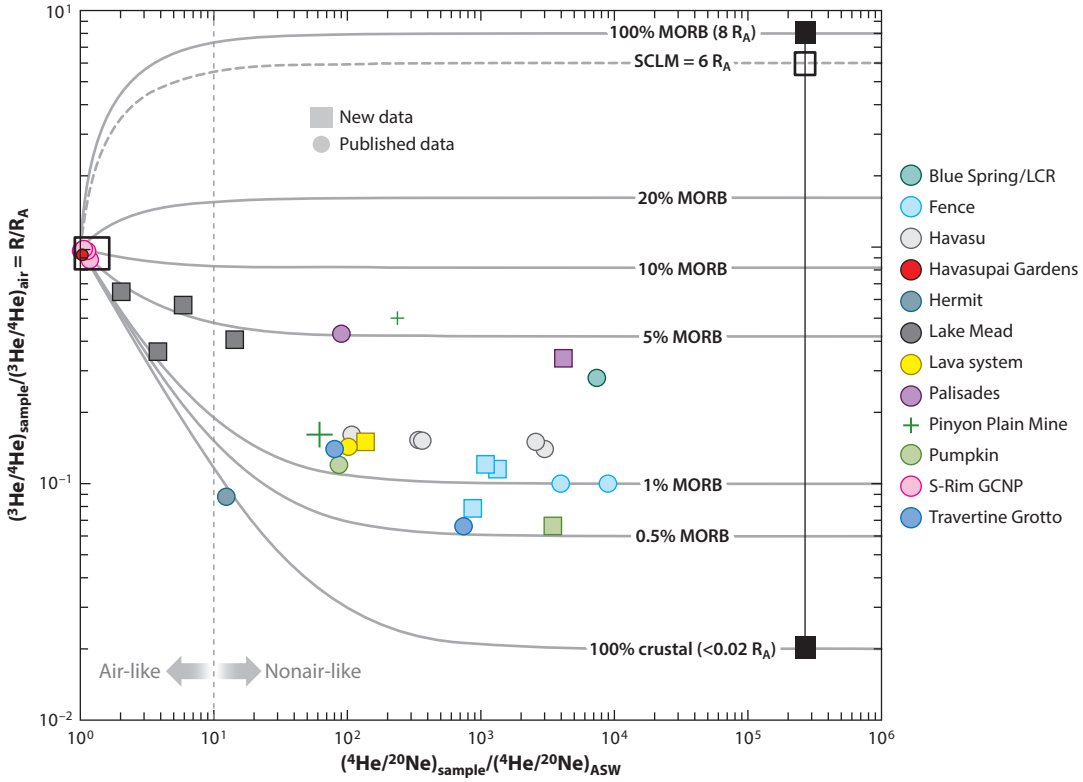

Figure 4

(*a*) $^3He/^4He$ isotope ratios providing evidence for mantle-derived fluid inputs. Square symbols are new data; round symbols are previously published data (**Supplemental Table 1**). After correction for air contamination using He/Ne, major travertine-depositing (CO_2-rich) springs in the Grand Canyon region show that from up to 5% (Palisades and Blue) to 0.5% (Pumpkin) of their total helium is derived from MORB-like mantle (Crossey et al. 2006) or a higher percentage using a SCLM (Solder & Beisner 2020). A second set of springs have air-saturated water values (and tritium); these are S-Rim springs that contain significant N-Rim pipeline water (Curry et al. 2023). Hermit Spring has values consistent with crustal (radiogenic) helium production of 0.02 R_A with no mantle component. Data are in **Supplemental Table 2**. Abbreviations: GCNP, Grand Canyon National Park; LCR, Little Colorado River; MORB, mid-ocean ridge basalt; R_A, $^3He/^4He$ in air ($\sim 1.384 \times 10^{-6}$); S-Rim, South Rim; SCLM, subcontinental lithospheric mantle.

S-Rim endogenic springs have nonair-like $^4He/^{20}Ne$ of >2.7 (10 times the mean ASW value), and $^3He/^4He > 0.02$ R_A, hence a quantifiable amount of mantle-derived helium (**Figure 4**; **Supplemental Table 2**). We do not apply an arbitrary cutoff between crustal and mantle values of 0.15 R_A (Solder et al. 2020). Instead, in keeping with continental-scale helium studies (Crossey et al. 2016, Klemperer et al. 2022), we interpret quantifiable mantle-helium percentages to have significance for both degrading water quality and showing tectonic influences. Mantle-derived gases in Grand Canyon springs range from up to 5% (Blue) to 0.5% (Pumpkin), and many springs have 1–2% of their total helium derived from a MORB source (Crossey et al. 2006) or a higher percentage assuming a SCLM source (Solder et al. 2020). Further, the Pinyon Plain Mine Observation Well value of ~2% mantle helium indicates vertical connectivity between deep fluids and the upper parts of the C aquifer where the well is screened. In contrast, S-Rim GCNP springs of Havasupai Gardens, Horn, Pipe, National, Grapevine, and 140-Mile have noble gas compositions similar to air-saturated water with no appreciable mantle helium, consistent with stable isotope evidence for young mixed-in N-Rim (pipeline) water. Hermit springs have values consistent

with dominantly crustal (radiogenic) helium production and pathways through the Precambrian basement, although only one of the samples has a slightly elevated $^{87}Sr/^{86}Sr$ value of 0.71152.

Cosmogenic isotope tracers ^{3}H (tritium) and ^{14}C can evaluate water sources, model ages, and mixing (Solder et al. 2020). However, these water age models are based on closed-system and piston-flow assumptions that do not adequately account for mixing. Nevertheless, we agree with some general conclusions of Solder et al. (2020). Springs containing ^{3}H greater than ~0.5 TU (tritium units) indicate mixing of a component of modern (post-1950s) recharge (of >4 TU; >12.8 pCi/L) with older (entirely pre-1950s) recharge (of <0.4 TU; <1.3 pCi/L) (Beisner et al. 2020). A post-1950s water component is found in Roaring Springs on the N-Rim that has 2.3–5.1 TU, values close to modern atmospheric levels (Ross 2005). Some of the S-Rim GCNP springs hypothesized to be sustained by N-Rim pipeline water have values of 1.8 TU (Horn Spring) to 0.8 TU (Pipe and Pumphouse springs) (Solder et al. 2020) that indicate a component of young recharge. Havasupai Garden spring (in the same spring system as Pumphouse) has no detected tritium, but the noble gas signature is close to air-saturated water (Solder et al. 2020) (**Figure 4**), suggesting a dominant component of fast-traveled young recharge. Importantly for understanding threats to groundwater, the observed modern water component in S-Rim GCNP springs and nearby Coconino Plateau wells indicates that both can respond in years-to-decades to groundwater additions, depletion, and contamination even though the majority of groundwater flow may be along longer flowpaths. Published models of distinct physical separation of a perched C aquifer above a regional R-M aquifer are at least partially incorrect due to underappreciated vertical connectivity.

^{14}C age models by Solder et al. (2020) show that S-Rim GCNP springs contain ^{14}C values with 17–130% modern ^{14}C (pMC) indicating the presence of a modern water component, in agreement with noble gases and tritium data. Quantification of a modeled age requires analytical correction methods to estimate the ^{14}C content of the total dissolved inorganic carbon ($^{14}C_{DIC}$) (Han & Plummer 2013). However, these model ages do not account for the extensive mixing that is documented by multiple tracers, and in carbonic waters, the hard water correction often does not account for the exceptionally high DIC because at pH values below 7, the carbonic acid component can be a significant component of DIC yet is not measured as alkalinity. Crossey et al. (2009) calculated total dissolved inorganic carbon (DIC_{tot}) using the speciation model PHREEQC (Parkhurst 1995) that considers pH, temperature, and measured alkalinity to estimate all components of the DIC (bicarbonate, carbonic acid, and carbonate) rather than just using measured alkalinity (Solder et al. 2020). DIC_{tot} in the endogenic waters can be an order of magnitude higher as the titration alkalinity does not include the significant amount of H_2CO_3 in carbonic waters. Based on water chemistry and C isotopes, in the high-volume S-Rim springs of Blue and Havasu, the percentage of the DIC_{total} that comes from soil contributions (C_{org}) is below ~25%; the proportions of dead (i.e., old) carbon from dissolving carbonate in the aquifer (C_{carb}) and carbon derived from lower world CO_2 (C_{endo}) are ~40% and >30%, respectively. Thus, the mixing of ^{14}C-rich fast-traveled meteoric recharge, karst aquifer baseflow, and deeply derived CO_2-rich waters is not addressed in the age model, leading to erroneously young ages. Nevertheless, if model ages (Solder et al. 2020) are used as a tracer and not interpreted as actual age, they help identify groups of springs with different flowpaths and mixing. For example, the S-Rim GCNP springs plot as a multi-variate cluster (Beisner et al. 2020, figure 10) having a significant younger water component consistent with mixing of N-Rim pipeline water with S-Rim groundwater. The Pinyon Plain Well and Pinyon Plain Observation Well have similar ^{14}C model ages, consistent with vertical connectivity between aquifers.

The simplified lumped parameter models (LPMs) of Solder et al. (2020) estimate mean age and age distribution, but the large number of assumptions required to fit their LPM models to

their tracer data gives low confidence in the age distribution results. They interpret the mean age as an age that has a high probability of being present, but this is not necessarily true in mixed waters. Reported results are empirically confusing: For example, the large range of mean ages of 175–19,100 years for nearby S-Rim springs is difficult to explain by different proportions of winter recharge (F_{win}) relative to summer recharge reaching individual and nearby springs (also the objection to their stable isotope meteoric recharge mixing model of **Figure 2*b***). The 14,000–19,000 model ages of Blue and Havasu springs systems and the 10,000–13,000 year estimates for the Coconino Plateau wells are all within one standard deviation and hence are not distinguishable from each other, as is also suggested by their similar stable isotope fingerprints. Young mean model ages for nearby S-Rim GCNP springs (e.g., Hermit, 6,150 years; Monument, 2,930 years; Havasupai Gardens, 87–2,750 years; Pipe, 1,047 years; Salt, 1,000 years; Lonetree, 710 years; and Horn, 356 years) seem best explained by mixing of N-Rim (pipeline) water infiltrating from the S-Rim Water Reclamation Plant. For the F_{win} stable isotope mixing model (Solder & Beisner 2020) and the ^{14}C age models (Solder et al. 2020), the chosen end members and model parameters need to be questioned and revised when mixing models return >100% of one of the end members.

MICROBIAL TRACERS

One of the Grand Canyon's mesothermal (cool but above ambient temperature) springs was sampled for microbial communities in the context of regional studies (Colman et al. 2014, Crossey et al. 2016). Culture-independent analysis of the microbial communities at spring vents yielded abundant bacterial and archaeal 16S ribosomal RNA (rRNA) gene sequences. Travertine Grotto exhibits microbial community compositions atypical of freshwater systems and a unique population of micro-organisms influenced by fluid mixing. Archaeal 16S rRNA genes were detected similar to a hydrothermal fluid clone from the marine setting of the Mariana Trench (Papm3A65) that is affiliated with the marine benthic group of Archaea. Travertine Grotto had unique genus-level populations, and its microbial richness was the highest of the 30 mesothermal springs that were sampled across the western United States (Colman et al. 2014). Crossey et al. (2016) used the term continental smokers for these springs as a tectonic and biologic analog to black-and-white smokers of oceanic ridge systems. This motivates the possibility of additional discovery of microbial systems in endogenic springs that bridge between surficial oxidizing conditions and the reduced subsurface biosphere. Another application of microbial analysis is through using microbial tracers associated with modern populations to determine recharge pathways and/or as indicators of endangered populations (environmental DNA) (Miller et al. 2000).

ANTHROPOGENIC INFLUENCES

An N-Rim tracer study using nontoxic fluorescent food dyes was initiated by GCNP in 2005 to investigate connectivity between sinkholes on the Kaibab uplift and GCNP's drinking water source at Roaring Springs. The results of these experiments provide direct evidence of recharge-to-discharge connectivity and flow timescales. Four different dyes were injected into four sinkhole locations just after snowmelt in 2015 and just before snowmelt in 2016 (Jones et al. 2018), with additional 2017 results reported by Tobin et al. (2021). Dye receptor sites were placed in numerous R-M springs (**Figure 5**). Instead of showing up in nearby Roaring Springs, the first dye, Eosin, was detected ~30 km to the east (Vasey's Spring) and west (Tapeats/Thunder/Deer) less than one month after injection. The 2016 injection of uranine was detected at Vasey's and Roaring and other springs in Bright Angel Creek within three months. Two of the 2015 dyes, phloxine B and sulfohodamine B, were not detected in any spring. The 2017 injection of uranine was detected in Fence, Nankoweap, and Roaring springs. The striking conclusion of this dye tracer study is

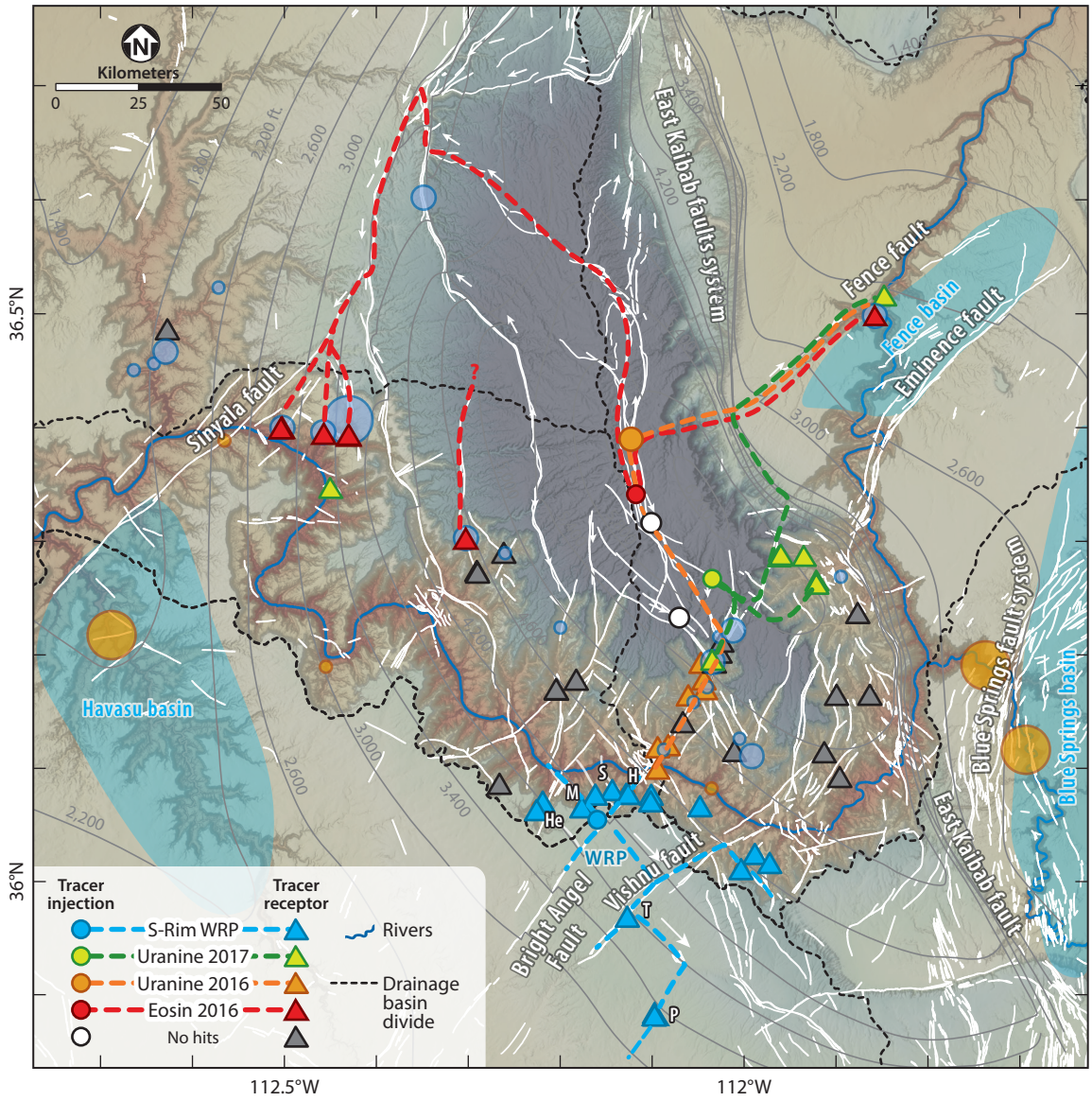

Figure 5

N-Rim dye tracer studies (Jones et al. 2018, Tobin et al. 2021) injected various dye tracers into sinkholes (*dots*); some reached detector locations (*triangles*) within weeks to months. On the S-Rim, pipeline water injected at the WRP along the Bright Angel fault is hypothesized to be affecting S-Rim springs and groundwaters based on using stable isotopes as time-averaged natural tracers (Curry et al. 2023). NW-trending faults mapped by Maxon (1968) may convey water to Hermit, Monument, Salt, Horn, and other S-Rim springs as well as to Tusayan and Pinyon Plain Mine wells. Structure contours (in feet) are drawn on the top of the Bright Angel Shale aquitard (adapted from Huntoon 2000). Fence, Blue Spring, and Havasu sub-basins on either side of the Kaibab uplift are in synclinal or graben depressions and are discharging from the upper Redwall, with the R-M aquifer filled; most other springs are discharging from the Muav, with the aquifer mostly drained. Data are in **Supplemental Table 1**. Abbreviations: H, Horn; He, Hermit; M, Monument; N-Rim, North Rim; P, Pinyon; R-M, Redwall-Muav; S, Salt; S-Rim, South Rim; T, Tusayan; WRP, Water Reclamation Plant.

that fast-traveled conduit flow takes place ~2 km vertically between the C and R-M aquifers plus ~30 km laterally in weeks to months at rates as much as 1 km/day, pushed by snowmelt pulses. **Figure 5** suggests that flow patterns for this fast-traveled portion of discharge were controlled by faults, as outlined conceptually by Huntoon (1974). Additional dye tracer studies are needed to refine how fault pathways and conduits can be built into future groundwater models.

On the S-Rim, an unintended tracer study has been conducted by GCNP during the ~60-year-long transcanyon pipeline experiment of N-Rim Roaring Springs water used and discharged from the Water Reclamation Plant along Bright Angel fault. **Figure 5** applies the Curry et al. (2023) model that stable isotope fingerprints can be used as a time-averaged natural tracer and suggests that springs directly below the S-Rim Village are sustained by tens of percents of N-Rim water (**Supplemental Table 1**). The fault network on the S-Rim is similar to the N-Rim such that fault conduits likely accelerate down-gradient flow from the Tusayan groundwater divide to Havasupai Gardens and other S-Rim GCNP springs (**Figure 1**). For example, transport from the S-Rim Water Reclamation Plant to Monument Spring, Horn Spring, and Salt Spring likely follows the NW-trending faults mapped by Maxon (1968) that connect the NE-trending Hermit and Bright Angel faults, forming an orthogonal grid of fast conduits. Anthropogenic tracers including pharmaceuticals and per- and polyfluoroalkyl substances (PFAS) found in Monument, Horn, and Pumphouse springs below Grand Canyon Village (Beisner et al. 2023b, Curry et al. 2023) help confirm the Curry et al. (2023) fault-connectivity model and show the need for continued monitoring given the time variability of hits, the minute quantities of pharmaceuticals and PFAS that can be detected, and pervasive human influences, even from hikers.

There are also anecdotal accounts of fast pathway connections to Havasu Springs. A regionally extensive flashflood in 1993 was reportedly swallowed by sinkholes and fissures in Cataract Creek on the S-Rim and showed up 65 km away at Havasu Springs two years later (Melis et al. 1996). At Grand Canyon Caverns (**Figure 1**), as the story goes, smoke released in the 1950s came out months later at Havasu Springs, 100 km to the north (Williams-Grand Canyon News 2001). The combined data pinpoint Havasu Springs, the most important water source for the Village of Havasupai, as among the most vulnerable high-discharge springs along the S-Rim.

SEISMICITY

Figure 6 shows the distribution of historical (1900–2011) seismicity from a variety of combined catalogs specific to Arizona (Lockridge et al. 2012, in supplement table S2). Earthquake magnitudes (M) were filtered to include only $M \geq 2.5$, the magnitude at which the USGS can typically detect and locate events in the contiguous United States (USGS 2018). This emphasis on the larger-magnitude events allows for a more objective comparison between records of seismic frequency before and during deployment of the Transportable Array (TA) across northern Arizona (2006–2009), which resulted in more small-magnitude detections. To avoid an artificial apparent decrease in seismicity after the TA, we focused on the historic catalog during and prior to 2006–2009. Earthquake intensity data, for historic events lacking magnitude estimates, were crudely scaled one-to-one (e.g., intensity of 3 = M3). Earthquake epicenter clusters occur around the San Francisco volcanic field, S-Rim Village, West Kaibab fault system, Toroweap, Hurricane, and Grand Wash fault systems (Brumbaugh 2005, 2008, 2019; Brumbaugh et al. 2014). The earthquakes record slip on a network of preexisting N-, NE-, and NW-striking faults of Laramide, Miocene, and Quaternary age. Focal mechanism solutions show normal faulting (Lay et al. 1994; Brumbaugh 2005, 2008; Wilgus & Brumbaugh 2014) with slip subparallel to dominant E-W geodetic extension (Kreemer et al. 2010a,b), indicating that preexisting faults are undergoing extensional reactivation.

The S-Rim Village area (**Figure 6*b***) epicenters include a mainshock–aftershock-type cluster of seismicity (Lockridge et al. 2012). Epicenters occur on and between the Hermit, Bright Angel and Vishnu faults, and several fault-cored Laramide monoclines. Focal mechanism solutions suggest that the ~NW-striking Laramide faults are being reactivated (Brumbaugh 2005). **Figure 6*c*** plots earthquakes through time and compares this record to cumulative pipeline pumping. Pipeline installation began in the 1960s, and water was pumped starting in the 1970s from Havasupai Gardens to S-Rim, delivering ~15 L/s (Lattimore et al. 1987). Pumping picked up to ~22 L/s in the 1980s,

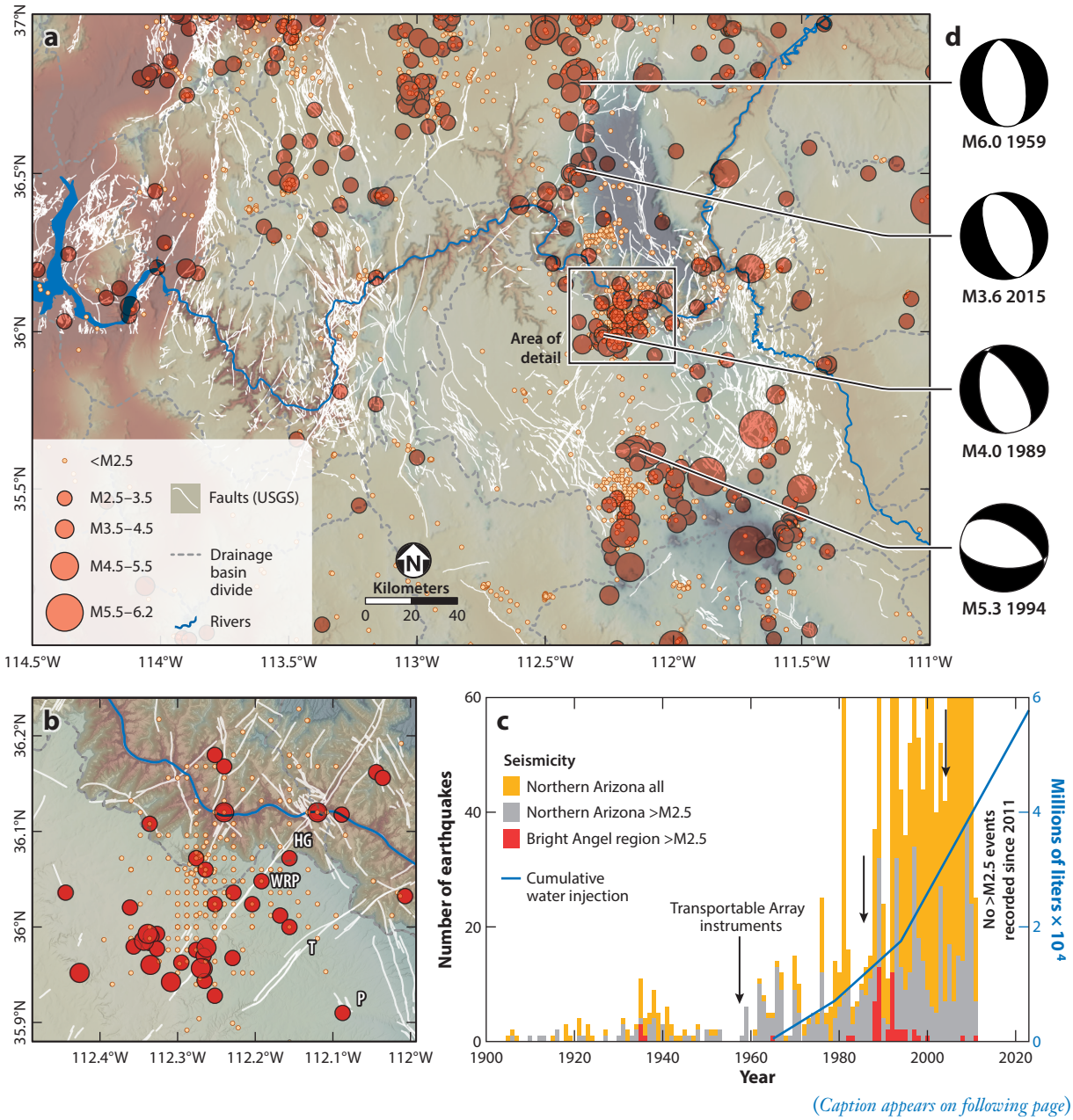

(*Caption appears on following page*)

Figure 6 (*Figure appears on preceding page*)

(*a*) Microseismicity of the Grand Canyon region (1900–2011) (Lockridge et al. 2012) with the black box highlighting the S-Rim earthquake cluster and mapped faults from Billingsley and colleagues (Billingsley & Hampton 2000; Billingsley & Priest 2013; Billingsley & Workman 2000; Billingsley et al. 2003, 2006a,b, 2007, 2008, 2013). (*b*) Enlargement of the S-Rim seismic cluster showing epicenters along NE- and NW-striking faults near S-Rim Village. Small earthquakes (*orange*) are only approximately located, giving an artificial grid pattern. (*c*) Seismicity through time in yearly bins suggesting that microseismicity apparently picked up around 1960, around the time of the first deployment of a seismic instrument in Arizona, again in ∼1990 a few years after the establishment of the Arizona Earthquake Information Center in 1986, and during deployment of Transportable Array seismic instruments (∼70-km spacing) from 2006 to 2009 (*black arrows*). The apparent increase in seismic frequency is likely in part related to better detection through time. However, implementing a magnitude threshold of 2.5 attempts to remove bias due to the increase in stations. The plot also shows approximate cumulative injection volumes at the S-Rim Village bracketed by average pipeline volumes and discharge at the WRP. (*d*) Focal mechanism solutions for representative earthquakes from Brumbaugh (2005) and Wilgus & Brumbaugh (2014) showing active extensional movement on a network of N-, NE-, and NW-striking normal faults. Abbreviations: HG, Havasupai Gardens; P, Pinyon Plain Mine; T, Tusayan wells; WRP, Water Reclamation Plant.

accompanied by a change in the Grand Canyon Village water distribution system when a diagonal pipeline was drilled. Water has been delivered to S-Rim at a rate of ∼44 L/s since 1995 (Natl. Park Serv. 1995). The question is whether the cumulative water infiltrated from S-Rim Village is enough to induce S-Rim seismicity at several-kilometer depths by lowering effective normal stress and allowing reactivation of older faults to relieve tensile stress. The extensive occurrence of highly charged carbonic springs may be an indicator of a system poised for seismic response such that relatively small hydrologic loads could serve as a trigger. Constraints on intrinsic permeability and more detailed characterization of the fault systems of the S-Rim Village area could help determine their suitability to host induced seismicity given the relatively small injection volumes (Talwani et al. 2007, Faulkner et al. 2010). An increase in seismic stations and monitoring in the Grand Canyon region would serve to establish a seismic baseline. If in fact seismicity is being induced, an S-rim focused microseismic study could provide the evidence (e.g., Glasgow et al. 2021).

URANIUM MINING AND THREATS

One of the threats to the regional groundwater system is contamination from uranium mining from breccia pipes that contain some of the richest uranium ores on Earth (Huntoon 1996; Tillman et al. 2021, 2023). A uranium mine on the S-Rim within GCNP (Orphan Mine) has been inactive for 50 years but is the most likely source of elevated uranium concentrations in Horn and Monument springs below the rim (Fitzgerald 1996, Liebe 2003, Monroe et al. 2005, Kreamer & Springer 2008). Pinyon Plain Mine (formerly Canyon Mine) about 15 km south of S-Rim resumed mining and extracting ore in January 2024 based on federal and Arizona state permits, but this is vigorously opposed by the Havasupai Tribe and others based on Indigenous knowledge of regional springs and groundwater. Our data support a public comment of David K. Kreamer that contaminants are highly likely to be transported between the C and R-M aquifers and regionally for several reasons. Stable isotope data, helium isotopes, and model ages at the Pinyon Plain Mine indicate the wells are likely to be hydrologically connected vertically between the local C and R-M aquifer, and laterally to other S-Rim springs and groundwaters (Curry et al. 2023). This was also shown during initial exploratory drilling that indicated variable water levels with most wells saturated through the Supai Group and hence likely to the underlying R-M aquifer (D.K. Kreamer, public comment). The unexpected 1.5 billion liters of artesian groundwater discharge from the C aquifer since 2013 (Reimondo 2020, Bane & Kruse 2021) refutes the APP application statements of lack of continuity and low groundwater storage in the C aquifer. The present two monitoring wells, one in the C aquifer and one in the R-M aquifer, have different stable isotope

signatures, indicating different waters, but two wells are inadequate to resolve direction and rate of groundwater flow or quantify contaminant transport (at least three wells would be required) (Hudak 2000).

At N-Rim sites, Beisner et al. (2017, p. 1) reported that "mining does not appear to explain the presence of elevated uranium concentrations in groundwater" based on an assumption of downgradient confined aquifer flow. But this was without considering unconfined vertical fracture flow from the Pigeon Mine to the nearby (lower elevation) Pigeon Spring that has high uranium concentrations (>50 μg/L). Tillman et al. (2021) concluded there are "no conclusive effects from breccia pipe mining activities on uranium concentrations in groundwater samples collected to date." But even though 95% of the groundwaters they analyzed met safety standards, they also reported that 8 of 11 uranium content exceedances are in proximity to breccia pipe mines. Our alternative conclusion of the USGS studies is that there is no conclusive evidence that breccia pipe mining does not affect groundwater uranium concentrations. Arsenic is also a societal concern. Tillman et al. (2023) state there is "limited evidence to-date of mining effects on elevated arsenic in groundwater," yet they show that "maximum arsenic concentrations exceed the [USEPA Maximum Contaminant Level of 10 μg/L] in springs near Orphan Lode Mine and the regional groundwater well at Pinenut Mine." These authors acknowledge that "few water-quality data are available from groundwater sites at or near uranium mining areas" and that there is a time factor of "decades or more for groundwater to reach discharge locations." We advocate a more conservative scientific management approach that acknowledges the demonstrated risks of vertical transport and fast flowtimes along fault pathways. The combined structural and tracer data show that the C aquifer is vertically connected to the R-M aquifer in many places and that both are affected by very fast transit of young waters along incompletely understood fault and karst conduit pathways that can amplify anthropogenic contamination and overuse. In our view, the protection of spring ecosystems and tribal water sources and sacred sites requires cessation of all uranium mining activities at Pinyon Plain Mine and perhaps others. Better monitoring using existing and additional wells near this site could make major scientific contributions to understanding Colorado Plateau hydrology and inclusion of traditional Indigenous knowledge about the region's springs and groundwater is also needed (Tilousi & Hinck 2024).

SYNTHESIS

Our hydrotectonic model involves fault-controlled groundwater sub-basins of the Grand Canyon region (**Figures 1** and **5**), each with unique hydrology and hydrochemistry resulting from structurally influenced mixing of water types, different flowpaths, and recharge ages. N-, NE-, and NW-striking faults are under active E-W extension, creating potential fast conduits. Breccia pipes and vertical fault intersections provide vertical connectivity that homogenizes waters between the C and R-M aquifers. Meteoric recharge from isotopically varied winter snowpack with highly variable summer monsoon meteoric recharge takes place on both rims, and the different stable isotope fingerprints for N-Rim and S-Rim groundwater reflect their different average recharge elevation. Infiltration and first-stage mixing take place in the karst/sandstone C aquifer; further mixing of water types and water ages takes place en route to and within the deeper R-M aquifer. Low-volume but geochemically potent geothermal fluids move up faults, which enhances hypogene karst development. The result is a significant ~1‰ temporal $\delta^{18}O$ hydrochemical variability in each spring within a >6‰ $\delta^{18}O$ regional variation. N-Rim Kaibab uplift-derived fast-traveled waters emerge from the Muav Formation at the base of the mostly drained R-M aquifer, indicating sensitivity to climate change (Lachniet et al. 2023) and decreasing snowpack (Tillman et al. 2020). S-Rim synclinal and graben sub-basins have springs that emerge from the upper Redwall Limestone from areas where the R-M aquifer is full, indicating greater baseflow storage and

helping explain higher TDS waters. Fault-bounded hydrologic sub-basins and their main high-discharge spring vents are located in different federal, tribal, state, and municipal jurisdictions and need collaborative monitoring to understand their degree of interconnectedness to assure future resilience and sustainability.

The six-decade-long anthropogenic transcanyon pipeline experiment of injecting N-Rim water at S-Rim may have the societally positive impact of sustaining S-Rim springs and groundwater as far away as Tusayan and the Pinyon Plane Mine. Induced microseismicity may also be beneficial in relieving stress buildup on faults and lowering the (already low) seismic hazard. The same data highlight the potential for contamination from the Pinyon Plain Mine to S-Rim GCNP springs and wells, especially the vulnerable down-gradient Havasu Springs near Havasupai Village. Continued multi-approach tracer studies are needed that involve dyes, natural tracers, other anthropogenic tracers, and enough time to see and quantify their flowpaths. Additional monitoring with more than two wells at the Pinyon Plain Mine and other mines is needed to test for contaminant changes.

DISCLOSURE STATEMENT

The authors are not aware of any affiliations, memberships, funding, or financial holdings that might be perceived as affecting the objectivity of this review.

ACKNOWLEDGMENTS

Support was provided by Grand Canyon National Park Research Permits. Partial funding came from National Science Foundation (NSF) grant 1914490 from the University of New Mexico Centers for Research Excellence in Science and Technology, NSF grant EAR-1955078 from the Sedimentary Geology and Paleobiology Program, and NSF grant EAR-0538304 from the Hydrological Sciences Program. We thank the Grand Canyon Resource office for multiple GRCA research permits since 1995. The Grand Canyon shares boundaries with three federally recognized tribes, and a total of 11 federally recognized tribes are traditionally associated with what is now Grand Canyon National Park and Baaj Nwaavjo I'tah Kukveni. We acknowledge the Native peoples on whose ancestral homelands we work, as well as the diverse and vibrant Native communities who make their home here today. We thank Kim Beisner and David Kreamer for useful discussions.

LITERATURE CITED

Bane L, Kruse A. 2021. *Keeping tabs on Canyon uranium mine*. Rep., Grand Canyon Trust, Flagstaff, AZ

Beisner KR, Davidson C, Tillman F. 2023a. Anthropogenic influence on groundwater geochemistry in Horn Creek Watershed near the Orphan Mine in Grand Canyon National Park, Arizona, USA. *Geochem. Explor. Environ. Anal.* 23(3):geochem2023-007

Beisner KR, Paretti NV, Jasmann JR, Barbar LB. 2023b. Utilizing anthropogenic compounds and geochemical tracers to identify preferential structurally controlled groundwater pathways influencing springs in Grand Canyon National Park, Arizona, USA. *J. Hydrol.* 48:101461

Beisner KR, Solder JE, Tillman FD, Anderson JR, Antweiler RC. 2020. Geochemical characterization of groundwater evolution south of Grand Canyon, Arizona (USA). *Hydrogeol. J.* 28(5):1615–33

Beisner KR, Tillman FD, Anderson JR, Antweiler RC, Bills DJ. 2017. *Geochemical characterization of groundwater discharging from springs north of the Grand Canyon, Arizona, 2009–2016*. Sci. Invest. Rep. 2017-5068, US Geol. Surv., Reston, VA. **https://doi.org/10.3133/sir20175068**

Belitz K, Fram MS, Lindsey BD, Stackelberg PE, Bexfield LM, et al. 2022. Quality of groundwater used for public supply in the continental United States: a comprehensive assessment. *ACS ES&T Water* 2(12):2645–56

Billingsley GH, Block DL, Dyer HC. 2006a. *Geologic Map of the Peach Springs 30′ × 60′ Quadrangle, Mohave and Coconino Counties, Northwestern Arizona*. US Geol. Surv. Map SIM 2900

Billingsley GH, Felger TJ, Priest SS. 2006b. *Geologic map of the Valle 30′ × 60′ quadrangle, Coconino County, northern Arizona*. US Geol. Surv. Map SIM 2895

Billingsley GH, Hampton HM. 2000. *Geologic map of the Grand Canyon 30′ × 60′ quadrangle, Coconino and Mohave Counties, northwestern Arizona*. US Geol. Surv. Map I-2688

Billingsley GH, Priest SS. 2013. *Geologic map of the Glen Canyon Dam 30′ × 60′ quadrangle, Coconino County, northern Arizona*. US Geol. Surv. Map SIM 3268

Billingsley GH, Priest SS, Felger TJ. 2007. *Geologic map of the Cameron 30′ × 60′ quadrangle, Coconino County, northern Arizona*. US Geol. Surv. Map SIM 2977

Billingsley GH, Priest SS, Felger TJ. 2008. *Geologic map of the Fredonia 30′ × 60′ quadrangle, Mohave and Coconino Counties, northwestern Arizona*. US Geol. Surv. Map SIM 3035

Billingsley GH, Stoffer PW, Priest SS. 2013. *Geologic map of the Tuba City 30′ × 60′ quadrangle, Coconino County, northern Arizona*. US Geol. Surv. Map SIM 3227

Billingsley GH, Wellmeyer JL. 2003. *Geologic map of the Mount Trumbull 30′ × 60′ quadrangle, Mohave and Coconino Counties, northwestern Arizona, version 1.2*. US Geol. Surv. Map I-2766

Billingsley GH, Workman JB. 2000. *Geologic map of the Littlefield 30′ × 60′ quadrangle, Mohave County, northwestern Arizona*. US Geol. Surv. Map I-2628

Bills DJ, Flynn ME, Monroe SA. 2007. *Hydrogeology of the Coconino Plateau and adjacent areas, Coconino and Yavapai Counties, Arizona*. Sci. Invest. Rep. 2005-5222, US Geol. Surv., Reston, VA. **https://doi.org/10.3133/sir20055222**

Bills DJ, Truini M, Flynn ME, Pierce HA, Catchings RD, Rymer MJ. 2000. *Hydrogeology of the regional aquifer near Flagstaff, Arizona, 1994–97*. Water-Res. Invest. Rep. 2000-4122, US Geol. Surv., Tucson, AZ. **https://doi.org/10.3133/wri004122**

Brown C. 2011. *Physical, geochemical, and isotopic analyses of Redwall-Aquifer springs, North Rim, Grand Canyon, Arizona*. MSc Thesis, North. Ariz. Univ., Flagstaff

Brumbaugh DS. 2005. Active faulting and seismicity in a prefractured terrane: Grand Canyon, Arizona. *Bull. Seismol. Soc. Am.* 95(4):1561–66

Brumbaugh DS. 2019. Seismotectonics of the Grand Wash Arizona area. *Bull. Seismol. Soc. Am.* 109(6):2277–87

Brumbaugh DS. 2008. Seismicity and active faulting of the Kanab-Fredonia area of the southern Colorado Plateau. *J. Geophys. Res.* 113(B5):B05309

Brumbaugh DS, Hodge BE, Linville L, Cohen A. 2014. Analysis of the 2009 earthquake swarm near Sunset Crater volcano, Arizona. *J. Volcanol. Geotherm. Res.* 285:18–28

Chambless HE, Springer AE, Evans M, Jones N. 2023. Deep-karst aquifer spring flow trends in a water limited system, Grand Canyon National Park. *Hydrogeol. J.* 31(7):1755–71

Colman DR, Garcia JR, Crossey L, Karlstrom KE, Jackson-Weaver O, Takacs-Vesbach T. 2014. An analysis of geothermal and carbonic springs in the western United States sustained by deep fluid inputs. *Geobiology* 12:83–98

Cooley ME, Harshbarger JW, Akers JP, Hardt WF. 1969. *Regional hydrogeology of the Navajo and Hopi Indian reservations, Arizona, New Mexico, and Utah*. Prof. Pap. 521-A:1-61, US Geol. Surv., Washington, DC

Craig H. 1961. Isotopic variations in meteoric waters. *Am. Assoc. Adv. Sci.* 133:1702–3

Crossey LJ, Karlstrom KE. 2012. Travertines and travertine springs in eastern Grand Canyon: What they tell us about groundwater, paleoclimate, and incision of Grand Canyon. In *Grand Canyon Geology: Two Billion Years of Earth's History*, ed. JM Timmons, KE Karlstrom, pp. 131–43. Boulder, CO: Geol. Soc. Am.

Crossey LJ, Fischer TB, Patchett PJ, Karlstrom KE, Hilton DR, et al. 2006. Dissected hydrologic system at the Grand Canyon: interaction between deeply derived fluids and plateau aquifer waters in modern springs and travertine. *Geology* 34:25–28

Crossey LJ, Karlstrom KE, Schmandt B, Crow RR, Colman DR, et al. 2016. Continental smokers couple mantle degassing and distinctive microbiology within continents. *Earth Planet. Sci. Lett.* 435:22–30

Crossey LJ, Karlstrom KE, Springer AE, Newell D, Hilton DR, Fischer T. 2009. Degassing of mantle-derived CO_2 and He from springs in the southern Colorado Plateau region—neotectonic connections and implications for groundwater systems. *Geol. Soc. Am. Bull.* 121(7–8):1034–53

Crow R, Karlstrom KE, Darling A, Crossey LJ, Polyak V, et al. 2014. Steady incision of Grand Canyon at the million year timeframe: a case for mantle-driven differential uplift. *Earth Planet. Sci. Lett.* 397:159–73

Curry BH, Crossey LJ, Karlstrom KE. 2023. The Grand Canyon National Park (USA) water corridor: water supply, water quality, and recharge along the Bright Angel Fault. *Hydrogeol. J.* 31:1773–94

Doelling HH, Blackett RE, Hamblin AH, Powell D, Pollock GL. 2000. Geology of Grand Staircase-Escalante National Monument, Utah. *Utah Geol. Assoc.* 28:1–43

Earthq. Hazards Program. 2023. National Earthquake Information Center. *U.S. Geological Survey*. **https://www.usgs.gov/programs/earthquake-hazards/national-earthquake-information-center-neic**

Errol L. Montgomery & Assoc. 1999. *Supplemental assessment of hydrogeologic conditions and potential effects of proposed groundwater withdrawal Coconino Plateau Groundwater Subbasin, Coconino County, Arizona*. Rep., US Dept. Agric., Scottsdale, AZ

Faulkner DR, Jackson CAL, Lunn RJ, Schlische RW, Shipton ZK, et al. 2010. A review of recent developments concerning the structure, mechanics and fluid flow properties of fault zones. *J. Struct. Geol.* 32(11):1557–75

Fitzgerald J. 1996. *Subsurface residence time and geochemical evolution of spring waters issuing from the South Rim Aquifer in the Eastern Grand Canyon Arizona*. MSc Thesis, Univ. Nevada, Las Vegas

Glasgow M, Schmandt B, Wang R, Zhang M, Bilek SL, Kiser E. 2021. Raton Basin induced seismicity is hosted by networks of short basement faults and mimics tectonic earthquake statistics. *J. Geophys. Res. Solid Earth* 126(11):e2021JB022839

Grand Canyon Natl. Park. 2023. *Grand Canyon National Park announces Transcanyon Waterline construction-related closures*. News Release, Sept. 18. **https://www.nps.gov/grca/learn/news/announcement-of-tcwl-construction-closures-september-2023.htm**

Grand Canyon Trust. 2023. Water. *Grand Canyon Trust*. **https://www.grandcanyontrust.org/waters**

Han LF, Plummer LN. 2013. Revision of Fontes & Garnier's model for the initial ^{14}C content of dissolved inorganic carbon used in groundwater dating. *Chem. Geo.* 351:105–14

Hudak PF. 2000. *Principles of Hydrogeology*. Boca Raton, FL: Lewis. 2nd ed.

Huntoon PW. 1968. *Hydrology of the Tapeats Amphitheater and Deer Basin, Grand Canyon, Arizona*. MS Thesis, Univ. Ariz., Tucson

Huntoon PW. 1970. *The hydromechanics of the groundwater system in the southern portion of the Kaibab Plateau, AZ*. PhD Diss., Univ. Ariz., Tucson

Huntoon PW. 1974. The karstic groundwater basin of the Kaibab plateau, Arizona. *Water Resour. Res.* 10:579–90

Huntoon PW. 1981. Fault controlled ground-water circulation under the Colorado River, Marble Canyon, Arizona. *Groundwater* 19(1):20–27

Huntoon PW. 1982. *The Ground Water Systems That Drain to the Grand Canyon of Arizona*. Laramie: Univ. Wyo.

Huntoon PW. 1996. Large basin ground water circulation and Paleo-reconstruction of circulation leading to uranium mineralization in Grand Canyon breccia pipes, Arizona. *Mt. Geol.* 33:71–84

Huntoon PW. 2000. Variability of karstic permeability between unconfined and confined aquifers, Grand Canyon region Arizona. *Environ. Eng. Sci.* 6(2):155–70

Ingraham N, Zukosky KA, Kreamer DK. 2001. The application of stable isotopes to identify problems in large-scale water transfer in Grand Canyon National Park. *Environ. Sci. Technol.* 35(7):1299–302

Johnson PW, Sanderson RB. 1968. *Spring flow into the Colorado River, Lees Ferry to Lake Mead, Arizona*. Rep. 34, Ariz. State Land Dept. Water Resour., Phoenix

Jones CJR, Springer AE, Tobin BW, Zappitello SJ, Jones NA. 2018. Characterization and hydraulic behavior of the complex karst of the Kaibab Plateau and Grand Canyon National Park, USA. *Geol. Soc. Lond. Spec. Publ.* 466:237–60

Jones NA, Hansen J, Springer AE, Valle C, Tobin BW. 2019. Modeling intrinsic vulnerability of complex karst aquifers: modifying the COP method to account for sinkhole density and fault location. *Hydrogeol. J.* 27(8):2857–68

Karlstrom KE, Crossey LJ. 2023. Our common geoheritage: the first 100 international geoheritage sites from the Basque Coast to Grand Canyon. *Boatman's Q. Rev.* 36:4–6

Karlstrom KE, Lee J, Kelley S, Crow R, Crossey LJ, et al. 2014. Formation of the Grand Canyon 5 to 6 million years ago through integration of older palaeocanyons. *Nat. Geosci.* 7:239–44

Keppel MN, Karlstrom KE, Crossey L, Love AJ, Priestley S. 2019. Evidence for intra-plate seismicity from spring-carbonate mound springs in the Kati Thanda–Lake Eyre region, South Australia: implications for groundwater discharge from the Great Artesian Basin. *Hydrogeol. J.* 28(1):297–311

Kessler JA. 2002. *Grand Canyon springs and the Redwall-Muav aquifer—comparison of geologic framework and groundwater flow models.* MS Thesis, North. Ariz. Univ., Flagstaff

Klemperer SL, Ping Z, Whyte CJ, Darrah TH, Crossey LJ, et al. 2022. Limited underthrusting of India below Tibet: ^{3}He/^{4}He analysis of thermal springs locates the mantle suture in continental collision. *PNAS* 119(12):e2113877119

Knight J, Huntoon PW. 2022. *Conceptual models of groundwater flow in the Grand Canyon region, Arizona*. Sci. Investig. Rep. 2022-5037, US Geol. Surv., Reston, VA. **https://doi.org/10.3133/sir20225037**

Kreamer DK, Springer AE. 2008. The hydrology of desert springs in North America. In *Aridland Springs in North America, Ecology and Conservation*, ed. LE Stevens, VJ Meretsky, pp. 35–48. Tucson: Univ. Ariz. Press

Kreamer DK, Stevens LE, Ledbetter JD. 2015. Groundwater dependent ecosystems: policy challenges and technical solutions. In *Groundwater: Hydrochemistry, Environmental Impacts, and Management Practices*, ed. SE Adelana, pp. 205–30. Hauppauge, NY: Nova

Kreemer C, Blewitt G, Bennett RA. 2010a. Present-day motion and deformation of the Colorado Plateau. *Geophys. Res. Lett.* 37(10):L10311

Kreemer C, Blewitt G, Hammond WC. 2010b. Evidence for an active shear zone in southern Nevada linking the Wasatch fault to the Eastern California shear zone. *Geology* 38(5):475–78

Lachniet MS, Du X, Dee SG, Asmerom Y, Polyak VJ, Tobin BW. 2023. Elevated Grand Canyon groundwater recharge during the warm Early Holocene. *Nat. Geosci.* 16:915–21

Lattimore GM, Carden RS, Fischer T. 1987. *Grand Canyon directional drilling and waterline project*. Paper presented at the SPE/IADC Drilling Conference, New Orleans, LA, March 15–18. **https://doi.org/10.2118/16169-MS**

Lay T, Ritsema J, Ammon CJ, Wallace T. 1994. Rapid source-mechanism analysis of the April 29, 1993 Cataract Creek ($M_w = 5.3$), northern Arizona earthquake. *Bull. Seismol. Soc. Am.* 84(2):451–57

Liebe D. 2003. *The use of the $^{234}U/^{238}U$ activity ratio for the characterization of springs and surface streams in Grand Canyon National Park, Arizona*. MSc Thesis, Hochsch. Tech. Wirtsch., Dresden, Ger.

Lockridge JS, Fouch MJ, Arrowsmith JR. 2012. Seismicity within Arizona during the deployment of the EarthScope USArray Transportable Array. *Bull. Seismol. Soc. Am.* 102(4):1850–63

Loughlin WD, Huntoon PW. 1983. *Compilation of available ground water quality data for sources within the Grand Canyon of Arizona*. Rep. PX821020883, US Natl. Park Serv., Grand Canyon, AZ

Mason JP, Kennedy JR, Macy JP, Gungle B. 2023. *Hydrologic framework and characterization of the Little Colorado River alluvial aquifer near Leupp, Arizona*. Sci. Invest. Rep. 2023-5052, US Geol. Surv., Reston, VA

Maxon JH. 1968. *Geologic Map of the Bright Angel Quadrangle, Grand Canyon National Park, Arizona*. Grand Canyon, AZ: Grand Canyon Nat. Hist. Assoc.

McGibbon C, Crossey LJ, Karlstrom KE. 2022. Fence springs system of Grand Canyon: insight into the karst aquifer system of the Colorado Plateau Region. *Hydrogeol. J.* 30(8):2379–98

McKee ED. 1969. Stratified rocks of the Grand Canyon. In *The Colorado River Region and John Wesley Powell*, pp. 23–58. Washington, DC: US Geol. Surv.

Melis TS, Phillips WM, Webb RH, Bills DJ. 1996. *When the blue-green waters turn red: historical flooding in Havasu Creek, AZ*. Sci. Invest. Rep. 96—4059, US Geol. Surv., Tucson, AZ

Metzger DG. 1961. *Geology in relation to water availability along the South Rim Grand Canyon National Park Arizona*. Water-Supply Pap. 1475-c, US Geol. Surv., Washington, DC

Miller MP, Buto SG, Susong DD, Rumsey CA. 2016. The importance of base flow in sustaining surface water flow in the Upper Colorado River Basin. *Water Resour. Res.* 52:3547–62

Miller MP, Stevens LE, Busch JD, Sorensen JA, Keim P. 2000. Amplified fragment length polymorphism and mitochondrial sequence data detect genetic differentiation and relationships in endangered southwestern USA ambersnails (*Oxyloma* spp.). *Can. J. Zool.* 78(10):1845–54

Mohammed AM, Crossey LJ, Karlstrom KE, Krishnamurthy RV, Kehew AE, et al. 2022. Mantle-derived fluids in the continental-scale Nubian aquifer. *Chem. Geol.* 608:121023

Monroe SA, Antweiler RC, Hart RJ, Taylor HE, Truini M, et al. 2005. *Chemical characteristics of ground-water discharge at selected springs, South Rim Grand Canyon, Arizona*. Sci. Invest. Rep. 2004-5146, US Geol. Surv., Reston, VA

Natl. Park Serv. 1995. *Trans-Canyon water pipeline*, Rep. HAER AZ-95, Natl. Park Serv., Denver, CO. **https://memory.loc.gov/master/pnp/habshaer/az/az0600/az0661/data/az0661data.pdf**

Ordens CM, McIntye N, Underschulltz JR, Ransley T, Moore C, Mallants D. 2020. Preface: advances in hydrogeologic understanding of Australia's Great Artesian Basin. *Hydrogeol. J.* 28:1–11

Parkhurst D. 1995. *Users Guide to PHREEQC: A Computer Program for Speciation, Reaction-Path, Advective-Transport, and Inverse Geochemical Calculations*. Reason, VA: US Geol. Surv.

Piper AM. 1944. A graphic procedure in the geochemical interpretation of water-analyses. *Eos Trans. Am. Geophys. Union* 25:914–28

Polyak VJ, Hill CA, Asmerom Y, Decker DD. 2017. A conceptual model for hypogene speleogenesis in Grand Canyon, Arizona. In *Hypogene Karst Regions and Caves of the World*, ed. A Klimchouk, AN Palmer, J De Waele, AS Auler, P Audra, pp. 555–64. Cham, Switz.: Springer

Porter R, Reid M. 2021. Mapping the thermal lithosphere and melting across the continental US. *Geophys. Res. Lett.* 48(7):e2020GL092197

Reimondo A. 2020. *Canyon Mine: why no uranium mine is "safe" for the Grand Canyon*. Rep., Grand Canyon Trust, Flagstaff, AZ

Ross LE. 2005. *Interpretive three-dimensional numerical groundwater flow modeling: Roaring Springs, Grand Canyon*. MSc Thesis, North. Ariz. Univ., Flagstaff

Rumsey CA, Miller MP, Schwarz GE, Hirsch RM, Susong DD. 2017. The role of baseflow in dissolved solids delivery to streams in the Upper Colorado River Basin. *Hydrol. Process.* 31:4705–18

Schindel GM. 2015. *Determining groundwater residence times of the Kaibab plateau, R-Aquifer using temperature, Grand Canyon National Park, Arizona*. MSc Thesis, North. Ariz. Univ., Flagstaff

Sharp Z. 2017. *Principles of Stable Isotope Geochemistry*. Upper Saddle River, NJ: Pearson. 2nd ed.

Solder JE, Beisner KR. 2020. Critical evaluation of stable isotope mixing end-members for estimating groundwater recharge sources: case study from the South Rim of the Grand Canyon, Arizona, USA. *Hydrogeol. J.* 28:1575–91

Solder JE, Beisner KR, Anderson J, Bills DJ. 2020. Rethinking groundwater flow on the South Rim of the Grand Canyon, USA: characterizing recharge sources and flow paths with environmental tracers. *Hydrogeol. J.* 28:1593–613

Springer AE, Schaller EM, Junghans KM. 2017. Local versus regional groundwater flow from stable isotopes at western North America springs. *Groundwater* 55(1):100–9

Stegner W. 1992. *Beyond the Hundredth Meridian: John Wesley Powell and the Second Opening of the West*. Lincoln: Univ. Nebraska Press

Stevens L, ed. 2023. *Springs of the World: Distribution, Ecology, and Conservation Status*. Flagstaff, AZ: Springs Steward. Inst.

Swanson RK, Springer AE, Kreamer DK, Tobin BW, Perry DM. 2021. Quantifying the base flow of the Colorado River: its importance in sustaining perennial flow in northern Arizona and southern Utah (USA). *Hydrogeol. J.* 29:723–36

Talwani P, Chen L, Gahalaut K. 2007. Seismogenic permeability, k_s. *J. Geophys. Res.* 112(B7):B07309

Tillman FD, Beisner KR, Anderson JR, Unema JA. 2021. An assessment of uranium in groundwater in the Grand Canyon region. *Sci. Rep.* 11:22157

Tillman FD, Beisner KR, Jones CJR. 2023. Arsenic in groundwater in the Grand Canyon region and an evaluation of potential pathways for arsenic contamination of groundwater from breccia pipe uranium mining. *PLOS Water* 2(6):e0000109

Tillman FD, Gangopadhyay S, Pruitt T. 2020. Recent and projected precipitation and temperature changes in the Grand Canyon area with implications for groundwater resources. *Sci. Rep.* 10:19740

Tobin BW, Springer AE, Ballensky J, Armstrong A. 2021. Caves and karst of the Grand Canyon World Heritage Site. *Z. Geomorphol.* 62(Suppl. 3):125–44

Tobin BW, Springer AE, Kreamer DK, Schenk E. 2018. Review: the distribution, flow, and quality of Grand Canyon Springs, Arizona (USA). *Hydrogeol. J.* 26:721–32

Tilousi C, Hinck JE. 2024. *Expanded conceptual risk framework for uranium mining in Grand Canyon watershed—inclusion of the Havasupai Tribe perspective*. Rep. 2023-1092, US Geol. Surv., Reston, VA. **https://doi.org/10.3133/ofr20231092**

USGS (US Geol. Surv.). 2018. *USGS National Hydrography Dataset Plus High Resolution (NHDPlus HR) for 4-digit Hydrologic Unit*. National Hydrography Dataset Plus High Resolution (NHDPlus HR), US Geol. Surv. **https://www.sciencebase.gov/catalog/item/57645ff2e4b07657d19ba8e8**

USGS (US Geol. Surv.). 2020. *National Water Information System: Mapper*. **https://maps.waterdata.usgs.gov/mapper/index.html**

Weiss R. 1971. Solubility of helium and neon in water and seawater. *J. Chem. Eng. Data* 16:235–41

Wilgus JT, Brumbaugh DS. 2014. *Seismicity and tectonics of the West Kaibab Fault Zone, AZ*. Presented at AGU Fall Meet., Dec. 15–19, San Francisco, Abstr. T13B-4641

Williams-Grand Canyon News. 2001. Peck discovers GC Caverns in 1927 on way to poker game. *Williams-Grand Canyon News*, June 13, **https://www.williamsnews.com/news/2001/jun/13/peck-discovers-gc-cavernsbrin-1927-on-way-to-poke/**

Wilson E. 2000. *Geologic framework and numerical groundwater models of the South Rim of the Grand Canyon, Arizona*. MSc Thesis, North. Ariz. Univ., Flagstaff

Wilson JW, Erhardt AM, Tobin BW. 2022. Isotopic and geochemical tracers of groundwater flow in the Shivwits Plateau, Grand Canyon National Park, USA. *Hydrogeol. J.* 30(2):495–510

Wood AJ, Springer AE, Tobin BW. 2020. Geochemical variability in karst-siliciclastic aquifer spring discharge, Kaibab Plateau, Grand Canyon. *Environ. Eng. Geosci.* 26(3):367–81

Zukosky K. 1995. *An assessment of the potential to use water chemistry parameters to define ground water flow pathways at Grand Canyon National Park, Arizona*. MS Thesis, Univ. Nevada, Las Vegas